



Hendry, K., & Brzezinski, M. (2014). Using silicon isotopes to understand the role of the Southern Ocean in modern and ancient biogeochemistry and climate. *Quaternary Science Reviews*, 89, 13-26. <https://doi.org/10.1016/j.quascirev.2014.01.019>

Peer reviewed version

Link to published version (if available):
[10.1016/j.quascirev.2014.01.019](https://doi.org/10.1016/j.quascirev.2014.01.019)

[Link to publication record in Explore Bristol Research](#)
PDF-document

University of Bristol - Explore Bristol Research

General rights

This document is made available in accordance with publisher policies. Please cite only the published version using the reference above. Full terms of use are available:
<http://www.bristol.ac.uk/red/research-policy/pure/user-guides/ebr-terms/>

- proxies reveal variations in the northward flow of Southern Ocean intermediate and mode waters and how changes in Southern Ocean productivity altered their preformed nutrient content. We present a new hypothesis – the “Silicic Acid Ventilation Hypothesis” (SAVH) – to explain the geographical variation of opal-based proxy records, in particular the contrasting patterns of opal burial change found in the low and high latitudes. By understanding the silicon isotope systematics of opal and silicic acid in the modern, we will be able to use opal-based proxies to reconstruct past changes in the Southern Ocean and so investigate its role in global carbon cycling and climate.

Keywords: silicon isotope, silicic acid, opal, diatom

1. Introduction

1.1 Background and motivation

The Southern Ocean plays a central role in governing the inventory of preformed nutrients and carbon storage in the global ocean (Marinov et al., 2008; Marinov et al., 2006). Of particular interest is the role of Southern Ocean circulation and biogeochemistry as a major control on the global distribution of the dissolved silicon - silicic acid or $\text{Si}(\text{OH})_4$ – and as the single largest locus of modern opal deposition on the seafloor (Cortese et al., 2004; Figure 1). The formation and burial of biogenic opal, amorphous silica, is the most important sink of $\text{Si}(\text{OH})_4$ in the modern oceans, and is formed predominantly by diatoms, a diverse group of photosynthetic protists from the Class Bacillariophyceae. Diatoms have an absolute requirement for $\text{Si}(\text{OH})_4$ and have evolved mechanisms for efficient Si uptake and metabolism (Martin-Jezequel et al., 2003). $\text{Si}(\text{OH})_4$ uptake by diatoms severely depletes dissolved Si from surface waters (Falkowski et al., 2004). As such, diatoms rely on upwelled waters with elevated $\text{Si}(\text{OH})_4$, thriving in ecosystems such as coastal and open ocean

upwelling zones, areas of deep winter mixing (such as the Southern Ocean frontal zones), and – in the case of some giant diatoms – obtaining their requisite silicon from deep nutriclines in highly stratified waters (Kemp et al., 2006).

Diatoms contribute up to 40% of global marine primary productivity, and approximately half of the opal produced in the euphotic zone is exported to deep waters (Nelson et al., 1995; Tréguer et al., 1995). Approximately 3% of biogenic opal production is preserved in ocean floor sediments as a global average (Nelson et al., 1995), with the remainder remineralized in the water column or at the sediment-water interface (reviewed by Tréguer and De la Rocha, 2013). Although the Southern Ocean is the single largest site of opal deposition (the “opal belt”) in the modern ocean (Cortese et al., 2004), opal preservation efficiency in the Southern Ocean is not significantly different from the global average (2-6%; DeMaster, 2002; Nelson et al., 2002; Pondaven et al., 2000) such that the high opal accumulation rates in Southern Ocean sediments is sustained by high rates of opal production rather than high preservation efficiency.

Diatom opal has received significant scrutiny over the past decades as a source of paleoceanographic information. Southern Ocean waters are often too corrosive for the preservation of traditional carbonate proxies, creating substantial interest in using opal as an indicator of past changes in southern component water. Opal accumulation rates, when ^{230}Th -normalised to account for sediment redistribution, provide an important constraint on the productivity and export of diatoms from surface waters into deep waters and sediments (Chase et al., 2003b). $^{231}\text{Pa}/^{230}\text{Th}$ ratios in opal-rich regions provide an additional constraint on opal production, versus preservation, due to the affinity of ^{231}Pa for opal (Chase et al., 2002). Given the dependence of diatoms on deep sources of Si(OH)_4 , ^{230}Th -normalised opal accumulation rates, paired with $^{231}\text{Pa}/^{230}\text{Th}$ ratios, have been used as a proxy for wind-driven upwelling in the Southern Ocean (Anderson et al., 2009).

76 In addition to opal accumulation, there has been an increasing interest in the last twenty years
77 on the use of aspects of opal chemistry as biogeochemical proxies for environmental
78 conditions and productivity, including elemental ratios of occluded trace constituents
79 (Ellwood and Hunter, 1999; Hendry and Rickaby, 2008; Lal et al., 2006) and stable isotopes
80 of Si (De La Rocha et al., 1997; De La Rocha et al., 1998), O (Leng and Sloane, 2008;
81 Shemesh, 1995), and more recently Zn (Andersen et al., 2011; Hendry and Andersen, 2013).
82 One of the widest used applications is that of Si isotope analysis of diatom opal as a proxy for
83 silica production. Briefly, there are three naturally occurring stable isotopes of silicon, ^{28}Si
84 (~ 92 atom %), ^{29}Si (~ 5 atom %) and ^{30}Si (~ 3 atom %), and the silicon isotope composition of
85 a material is denoted by $\delta^{30}\text{Si}$, where:

$$86 \quad \delta^{30}\text{Si} = [({}^{30}\text{Si}/{}^{28}\text{Si})_{\text{sample}}/({}^{30}\text{Si}/{}^{28}\text{Si})_{\text{standard-NBS28}} - 1] \times 1000 \quad (1)$$

87 De La Rocha and co-workers first reported on the fractionation of isotopes of Si by
88 diatoms using laboratory cultures (De La Rocha et al., 1997). That work indicated that
89 diatoms have a constant fractionation factor (ϵ) favouring the lighter isotope ^{28}Si over ^{30}Si by
90 ~ 1.1 ‰, with similar results achieved a few years later in further culture studies (Milligan et
91 al., 2004) and field observations of water column diatoms (Fripiat et al., 2012; Fripiat et al.,
92 2011; Varela et al., 2004), but see Sutton et al (2013) for evidence for possible interspecific
93 variation in ϵ (see below). Hence, as $\text{Si}(\text{OH})_4$ utilization increases, both dissolved silicic acid
94 and the opal produced from it become progressively enriched in the heavier isotopes of Si,
95 such that the silicon isotopic composition of diatom opal extracted from dated sediment cores
96 can be used as a measure of past surface ocean Si utilization. These concepts were first
97 applied to downcore records of diatom $\delta^{30}\text{Si}$ from the Southern Ocean (De La Rocha et al.,
98 1998). This progressive fractionation can be modelled as a Rayleigh-type closed distillation
99 process, or a steady state open system, assuming a constant value of ϵ and a known starting

isotopic composition of the nutrient substrate (De La Rocha et al., 1997; Varela et al., 2004).

The aim of this review is to bring together advances in oceanic silicon isotope studies with a focus on the role of Southern Ocean circulation and productivity in controlling the global distribution of Si(OH)_4 and the contribution of diatoms to global marine productivity. We will explore controls on Si isotope distribution deduced from models of modern oceanic $\delta^{30}\text{Si(OH)}_4$ distributions, the application of Si isotopes to paleoceanographic studies of Earth's climate, using the Silicic Acid Leakage Hypothesis (SALH) as a case study, and the future of opal-based multi-proxy approaches in paleoceanography.

2. Silicon isotopes as a silica production proxy

2.1. Culture experiments on diatoms

Since the original studies of De la Rocha et al. (1997) and Milligan et al. (2004), there was a considerable gap before further laboratory culture studies were carried out, which ended only recently with the publication of new culture experiments by Sutton et al. (2013). These culture experiments used the same species as the original studies (*Thalassiosira weissflogii* and *T. pseudonana*, De La Rocha et al., 1997; Milligan et al., 2004), and some Southern Ocean species that had not been previously studied (*Porosira glacilis*, *T. antarctica*, *T. nordenskioeldii*, *Fragilariopsis kerguelensis*, *Chaetoceros brevis*). Most of the results were consistent with the original findings (Figure 2), supporting the paradigm that diatom ϵ has a value of -1.1 ‰ within experimental uncertainty. However, there were some discrepancies between the different studies for different strains of the same species, *T. weissflogii*. Furthermore, two polar species had significantly different fractionation factors: *F. kerguelensis* showed a ϵ value of -0.54 ‰ (mean for two strains) and *C. brevis* showed a ϵ value of -2.09 ‰ (Sutton et al., 2013). Two major questions arising from these studies are: Do the results of culture experiments capture the range of fractionation by diatoms in the

natural environment? And, is interspecific variation in ϵ , as represented by the extreme value for *C. brevis*, detectable in nature?

2.2. Proxy verification: Core top calibrations of diatoms

2.2.1. Cleaning methods

An important aspect of paleoceanographic applications of opal composition is the effective cleaning of frustules to remove clays and fragments of other biogenic opal producers (radiolarians, sponge spicules). Heavy liquid separation has been used routinely for opal analysis for over twenty years, but there are numerous different approaches for further physical and chemical cleaning of the opal prior to analysis (Ellwood and Hunter, 1999; Hendry and Rickaby, 2008; Lal et al., 2006; Shemesh, 1989). Most studies of diatom Si isotopes have employed variants on these more traditional methods. Most recently, a microfiltration method originally designed to separate different species of coccoliths from sediments (Minoletti et al., 2009) has recently been adapted for the cleaning and separation of different size fractions of opal (Egan et al., 2012). The gentle sonication of the samples limits the potential for frustule fragmentation and thus mechanical loss of material. The studies show that size fractions for core tops in the Southern Ocean between 2-20 μm contain only clean diatom opal and yield reproducible $\delta^{30}\text{Si}$ values. Fractions below and above this range show $\Delta\delta^{30}\text{Si}$ offsets: <2 μm contain unidentifiable fragments whereas fractions >20 μm contain identifiable fragments of sponge spicules and radiolarians.

There are some potential issues relating to size fractionation of opal samples. Firstly, although the microfiltration method is designed to limit the fragmentation and loss of material, it is still inevitable that material will be lost during the heavy liquid separation stage, any further filtration stages and during chemical cleaning. Secondly, selective loss of more fragile frustules, and size selection of different species, may both reduce apparent variability and introduce a bias into the measurement, for example, towards species that grow at a

particular time of year or a particular ambient Si(OH)_4 condition. However, the few studies that have been carried out on hand-picked individual frustules of particular species have shown little offset with bulk opal $\delta^{30}\text{Si}$ values (e.g. Hendry et al., in press).

2.2.2. Core top calibration results

As alluded to above, one key point to address is whether the opal $\delta^{30}\text{Si}$ signal from diatoms in the upper parts of the water column is preserved with fidelity in the sediments. To address this Egan et al. (2012) carried out the first core top calibration of diatom $\delta^{30}\text{Si}$ using the microfiltration method. The authors found a good correspondence between the core top diatom $\delta^{30}\text{Si}$ from the 2-20 μm size fraction and the minimum annual Si(OH)_4 in the overlying surface waters, which, assuming the same initial Si(OH)_4 concentration everywhere at the end of winter should reflect the extent of Si(OH)_4 depletion. This result suggests that the sedimentary signal reflects the cumulative seasonal drawdown of Si(OH)_4 supporting the use of $\delta^{30}\text{Si}$ as a production proxy (Egan et al., 2012). Moreover, these data imply that species composition does not impact the $\delta^{30}\text{Si}$, once the opal from radiolarians and sponge spicules has been removed. The calculated ϵ values from the core tops appear to be greater when modelled at steady state from a single source of water (Figure 2). However, the core top results are compatible with an ϵ value of -1.1 ‰ if fractionation occurs from waters with a $\delta^{30}\text{Si(OH)}_4$ composition that lies on a mixing line representing a varying mixture of isotopically heavy surface water and lighter deep water in the Southern Ocean (Egan et al., 2012).

2.3. Field estimates of the Si fractionation factor

Field estimates of the fractionation factor ϵ have been made using either the gradient in the isotopic composition of silicic acid across the nutricline, or from the difference between the isotopic composition of co-located samples of biogenic silica and dissolved silicon.

173 Nutrient and isotope profiles can be used to estimate isotope fractionation using either an
 174 open system model (continuous delivery of Si into the euphotic zone) or a closed system
 175 model (assuming one isolated pulse of Si delivered into the euphotic zone followed by closed
 176 system dynamics) depending on the nature of the vertical nutrient supply. These models are
 177 described by the following equations:

$$178 \quad \text{Open: } \delta^{30}\text{Si}(\text{OH})_{4\text{observed}} = \delta^{30}\text{Si}(\text{OH})_{4\text{initial}} - \epsilon * (1 - f) \quad (2a)$$

$$179 \quad \text{Closed: } \delta^{30}\text{Si}(\text{OH})_{4\text{observed}} = \delta^{30}\text{Si}(\text{OH})_{4\text{initial}} + \epsilon * \ln(f) \quad (2b)$$

180 where $\delta^{30}\text{Si}(\text{OH})_{4\text{observed}}$ is the measured $\delta^{30}\text{Si}(\text{OH})_4$ in surface waters, $\delta^{30}\text{Si}(\text{OH})_{4\text{initial}}$ is that
 181 of the water mass supplying Si to surface waters and f is the fraction of the supply that
 182 remains in surface waters. Simple algebra can be used to show that surface water $\delta^{30}\text{Si}(\text{OH})_4$
 183 should be a linear function of $[\text{Si}(\text{OH})_4]_{\text{observed}} / [\text{Si}(\text{OH})_4]_{\text{initial}}$ (open) or $\ln[\text{Si}(\text{OH})_4]_{\text{observed}}$
 184 (closed) with a slope equal to ϵ (Varela et al. 2004).

185 In both the open and closed isotope models the $\delta^{30}\text{Si}(\text{OH})_4$ of waters ventilating to the
 186 surface is required. Uncertainty in this value has led to considerable variations in estimates of
 187 ϵ (Reynolds et al., 2006) inspiring efforts to better understand $\delta^{30}\text{Si}(\text{OH})_4$ distributions in
 188 subsurface waters.

189 In principle, ϵ can also be estimated from the difference between $\delta^{30}\text{Si}$ of opal and
 190 $\delta^{30}\text{Si}(\text{OH})_4$, a parameter denoted by $\Delta\delta^{30}\text{Si}$ (Cardinal et al., 2005; De La Rocha et al., 2011;
 191 Fripiat et al., 2007). Equating $\Delta\delta^{30}\text{Si}$ and ϵ is only approximate due to the influence of
 192 vertical mixing of isotopically light $\text{Si}(\text{OH})_4$ altering the biologically-driven relationship
 193 between $\delta^{30}\text{Si}$ of opal and $\delta^{30}\text{Si}(\text{OH})_4$.

194 A summary of the values of ϵ from field programs is given in Figure 2. The range of
 195 estimated fractionation factors reflects both real-world variation in ϵ and methodological

challenges. Often the simple assumptions made when applying isotope models are violated in natural systems. No system is entirely closed or entirely open causing ambiguity in the correct choice of which isotope model to apply with mixing, also biasing $\Delta\delta^{30}\text{Si}$ as described above.

In polar regions, biological production associated with seasonal sea ice adds additional complexity to silicon isotope dynamics. In the open waters of the Southern Ocean the limited data available suggest that the isotopic composition of opal sinking to depth reflects patterns in the diatom $\delta^{30}\text{Si}$ from the mixed layer (Varela et al., 2004; Fripiat et al., 2012). However, within the relatively closed sea-ice environment of the Antarctic Sea-ice Zone, sea-ice diatoms become distinctly heavy (Fripiat et al., 2007). In that study the unique isotopic signature of the sea ice flora was not detected in the bulk opal signal from the open waters; however, Varela et al (unpublished) found a significant positive correlation between the isotopic composition of opal and the percent ice cover in the Canadian Basin of the Arctic Ocean suggesting a significant contribution of sea ice diatoms to the isotopic signature of opal in open water. Given the importance of sea ice dynamics in polar oceans resolving the contribution of the unique sea ice flora to the silicon isotope dynamics remains an outstanding challenge.

2.4. Other pelagic biogenic opal producers

In addition to diatoms, other organisms produce biogenic opal, including heterotrophic single-celled radiolarians (supergroup Rhizaria) that live throughout the water column, choanoflagellates (family Acanthoecidae) and silicoflagellates. Considerably less work has been carried out on Si isotope fractionation by radiolarians compared to diatoms (for some discussion, see Egan et al., 2012; Hendry et al., in press; Wu et al., 1997) and, currently, nothing is known about Si fractionation by silicoflagellates or choanoflagellates.

3. Silicon Isotopes in Sponge spicules as a silicic acid concentration proxy

Whilst sponges are generally considered less important than diatoms to the oceanic Si budget, recent studies suggest that they may contribute more than previously thought to the global uptake of Si(OH)_4 (Maldonado et al., 2011). Sponges are simple filter feeding benthic animals (Animalia; Porifera), without tissue grade of organisation. Skeletal support is provided by spicules, formed from proteins, carbonate or – in the case of Classes Demospongea and Hexactinellida – opal. Sponge spicule $\delta^{30}\text{Si}$, which has a greater range and is isotopically light compared to diatoms (Egan et al., 2012), was first discussed as a potential paleoproxy a decade ago (De La Rocha, 2003). Following on from this study, two Southern Ocean calibration studies were published (Hendry et al., 2010; Wille et al., 2010), which showed the same relationship between fractionation factor (under equilibrium conditions $\epsilon \sim \Delta\delta^{30}\text{Si}$, ranging from -1 to -5 per mil) and Si(OH)_4 (Hendry et al., 2011), according to Equation 3 (Hendry & Robinson, 2012):

$$\Delta\delta^{30}\text{Si} = -6.54 + \frac{270}{53 + [\text{Si(OH)}_4]} \quad (3)$$

The lack of an apparent relationship between $\delta^{30}\text{Si}$ in spicules and species or temperature, pH, salinity, etc., suggests that spicules, from different ocean basins, may provide a robust proxy for past bottom water Si(OH)_4 concentrations (Figure 3; Hendry & Robinson, 2012). The non-linear relationship between $\Delta\delta^{30}\text{Si}$ and Si(OH)_4 concentration is likely a result of a uptake rate effect, whereby fractionation involved with uptake processes also becomes enhanced as Si uptake rates increase with concentration (Hendry and Robinson, 2012; Wille et al., 2010).

The ability of isotopes of Si to provide estimates of relative Si(OH)_4 depletion in surface waters (diatom $\delta^{30}\text{Si}$) together with estimates of the concentration of Si in ventilating waters (sponge $\delta^{30}\text{Si}$) makes $\delta^{30}\text{Si}$ unique among the paleo nutrient proxies. Knowing both the concentration of Si(OH)_4 in upwelled waters and the fraction of that Si supply that is

utilized in surface waters offers the possibility of estimating absolute silica production rates in the past.

4. Challenges and Caveats

4.1. *Is there such a thing as a constant fractionation factor?*

In order to fully understand the fractionation occurring during the biomineralization of Si, further work needs to be conducted on understanding the biochemical pathways involved in biosilicification. This is challenging as the biochemistry of biosilicification is largely unknown making it difficult to obtain a mechanistic understanding of how Si isotope fractionation arises in both diatoms and sponges. The fractionation of Si isotopes can potentially occur at several stages of the biosilicification process: uptake of Si(OH)₄ from seawater; polymerisation of SiO₂ within the Silica Deposition Vesicle (SDV); and efflux of excess Si from the cell. In diatoms, the efflux of Si does not impact ε (Milligan et al., 2004), which suggests that efflux does not discriminate among isotopes of Si.

The cumulative effect of these processes can be modelled for sponges assuming the fractionation occurs in several steps: firstly as the Si is transported into the cell, secondly as the Si is polymerized, and thirdly as Si is lost from the cell. The fractionation process can be expressed mathematically following Milligan et al., 2004:

$$\Delta\delta^{30}\text{Si} = \varepsilon_f = \varepsilon_{it} + (\varepsilon_p - \varepsilon_{ie}) \frac{v_E}{v_I} \quad (4)$$

Where ε_f = the total Si isotopic fractionation factor, ε_{it} = Si isotopic fractionation associated with transport into the cell, ε_p = Si isotopic fractionation associated with polymerization and ε_{ie} = Si isotopic fractionation associated with transport out of the cell; v_E = rate of Si efflux and v_I = rate of Si influx:

$$\varepsilon_f = \varepsilon_{il} + \Delta\varepsilon_p \left\{ 1 - \frac{\frac{v_{\max p}}{\left(\frac{K_{mp}}{[Si(OH)_4]} \right) + 1}}{\frac{v_{\max t}}{\left(\frac{v_{\max t} \times K_{mp} / v_{\max p}}{[Si(OH)_4]} \right) + 1}} \right\} \quad (5)$$

where $\varepsilon_p = (\varepsilon_p - \varepsilon_{tE})$; K_m are the half saturation constants and v_{\max} are the maximum incorporation rates. In the case of sponges, the half saturation constant and maximum incorporation rate for polymerization have been investigated in two sets of experiments and were found to be 46.41 μM and 19.33 $\mu\text{mol h}^{-1} \text{g}^{-1}$ (dry weight) based on explants i.e. tissue transferred to laboratory culture (Reincke and Barthel, 1997) or 74 μM and 1.7 $\mu\text{mol h}^{-1} \text{g}^{-1}$ (dry weight) based on whole specimens (Maldonado et al., 2011). The mathematical solution of Eq. 5 produces non-zero values for the fractionation associated with uptake, efflux and deposition (Hendry & Robinson, 2012). Application of a similar model to diatoms is challenging in the case of diatom field studies due to the difficulties in deconvolving apparent changes in ε due to water mass mixing (Egan et al., 2012), species variation (Sutton et al., 2013), or a possible environmental control on diatom ε as there is for sponges (Hendry & Robinson, 2012).

There have been recent developments in mixed layer modelling approaches to investigate possible mechanisms behind the apparent variation in diatom ε . Classic Rayleigh or steady state fractionation models, assuming a constant ε and a uniform upwelling water starting composition, fail to capture the range of apparent ε in the modern ocean, or the greater ε estimated from core tops (Egan et al., 2012). However, these can be reconciled in a number of ways: i) modelling uptake from waters with $\delta^{30}\text{Si(OH)}_4$ compositions that lie on

286 mixing lines between different water masses (as discussed above, Egan et al., 2012); ii)
287 modelling mixed layer processes that occur in the Southern Ocean to take into account higher
288 dissolution rates relative to opal production, and greater supply of Si(OH)_4 relative to the
289 uptake by diatoms (Fripiat et al., 2012).

290 ***4.2. Alteration of the production signal by fractionation during silica dissolution***

291 One of the most significant outstanding questions in understanding the marine silicon
292 cycle, and the role of the Southern Ocean in the distribution of Si(OH)_4 and silicon isotopes,
293 is the impact of dissolution of biogenic opal on apparent isotopic fractionation as this process
294 removes 97% of surface-produced opal leaving only 3% buried in the sediment record. There
295 has been only one published laboratory study addressing Si isotope fractionation during opal
296 dissolution, based on mixed-assemblage plankton trawl and sediment trap samples from the
297 Southern Ocean (Demarest et al., 2009). The dissolution of this material under controlled
298 conditions preferentially released the lighter isotopes of Si with a fractionation factor of -0.55
299 ‰. This would suggest that the progressive dissolution of sinking opal would result in a
300 trend towards increasing $\delta^{30}\text{Si}$ within opal with depth. The limited data on the isotopic
301 composition of suspended opal with depth in the water column (e.g. Fripiat et al., 2012), and
302 the limited core top studies of biogenic opal (Egan et al., 2012; Wetzel et al., in review), show
303 no indication of this trend. One hypothesis to explain this apparent discrepancy is that the
304 dissolution of opal is not congruent among frustules with the majority of frustules found at
305 depth or buried in sediments being relatively well preserved (note that <30% opal loss results
306 in a non-detectable change in $\delta^{30}\text{Si}$, Demarest et al., 2009) with the remainder being nearly
307 completely dissolved. Nelson et al (2002) found that in the Southern Ocean the opal that
308 survives dissolution in the upper 1,000 m is nearly entirely delivered to the sea floor,
309 consistent with the lack of changes in opal $\delta^{30}\text{Si}$ over this depth range in the Southern Ocean
310 (Fripiat et al., 2012).

A dichotomy between frustules that completely dissolve and those that are well preserved would largely eliminate the effect of dissolution in the water column from the sediment record. However, other factors may be involved. Preliminary data on fractionation of frustules recovered from sediments show little sign of fractionation during dissolution in seawater (Beucher & Brzezinski, unpublished) suggesting the possibility of fundamental differences in the effect of dissolution on fresh (Demarest et al, 2009) and preserved opal. Other sedimentary processes such as precipitation of Si on diatom frustules (Ren et al., 2013) have yet to be explored, along with the possibility of isotopic exchange with the high concentrations of silicic acid in pore waters. It is clear that the question of the impact of dissolution and abiotic precipitation/ isotope exchange on $\delta^{30}\text{Si}$ signatures must be addressed with further studies of monospecific diatom cultures and different types of biogenic silica (diatoms, sponges, radiolarians etc.) from different sources (fresh, preserved).

5. Southern Ocean Influence on the Modern $\delta^{30}\text{Si}(\text{OH})_4$ distribution

Dynamics in the Southern Ocean are a major control on the distribution of $\text{Si}(\text{OH})_4$, and its isotope composition, on a global scale. South of the SACCF (Antarctic Divergence) upwelled waters flow poleward and subduct with little biological removal of $\text{Si}(\text{OH})_4$ resulting in the high dissolved Si concentrations of Circumpolar Deep Water (CDW) and Antarctic Bottom Water (AABW) (e.g. Marinov et al., 2006). North of the Divergence Ekman transport is equatorward and biological productivity is strong. Diatoms remove a high fraction of the dissolved Si from surface waters, then sink with a portion of frustules dissolving into the southward propagating deeper waters, returning to the Divergence as dissolved $\text{Si}(\text{OH})_4$. This recycling loop traps $\text{Si}(\text{OH})_4$ in the Southern ocean water column. Frustules that escape dissolution accumulate on the sea floor forming the Southern Ocean opal belt, which – in the modern ocean – is the largest single locus of opal accumulation in the sea and is located within the Antarctic sector of the Southern Ocean to the south of the

336 Polar Front.

337 Antarctic Intermediate Water (AAIW) and Sub-Antarctic Mode Water (SAMW) form by a

338 combination of deep winter convection between the Polar Front and the Subantarctic Front

339 (Bostock et al., 2013) and wind-driven mixing (Holte et al., 2012), forming the northward

340 flowing shallow limb of the Meridional Ocean Circulation (MOC). AAIW and SAMW

341 (collectively referred to as Southern Ocean Intermediate Waters, SOIW, after Pena et al.,

342 2013) contain at least 10-15 μM silicic acid, but are depleted in $\text{Si}(\text{OH})_4$ relative to other

343 macronutrients (nitrate and phosphate), and it is these relatively low-silicon Mode Waters that

344 feed into the thermocline in the lower latitudes. This can be traced by the parameter Si^* ,

345 where $\text{Si}^* = [\text{Si}(\text{OH})_4] - [\text{NO}_3^-]$. SOIW have negative Si^* values, which can be seen far into the

346 North Atlantic, Indian and Pacific Oceans (Sarmiento et al., 2004).

347 There has been recent attention paid to the role of MOC in oceanic silicon isotope

348 distribution (de Souza et al., 2012a; de Souza et al., 2012b). In the high latitudes, in

349 particular the Southern Ocean, uptake of the lighter isotopes of Si by diatoms imparts a heavy

350 isotope signature (up to +2‰) in surface waters during the growth season, which is thought to

351 be preserved in the winter mixed layer. The heavy isotope signature is transferred to the

352 global thermocline via Mode Waters ($\delta^{30}\text{Si}(\text{OH})_4 \sim +1.8\text{‰}$), and mixed into North Atlantic

353 Deep Water (NADW, $\delta^{30}\text{Si}(\text{OH})_4 \sim +1.6\text{‰}$) (Cardinal et al., 2005; Cardinal et al., 2007; de

354 Souza et al., 2012b; Hendry et al., 2010). This is in contrast to deep waters in the Southern

355 Ocean and Pacific, which have lighter $\delta^{30}\text{Si}(\text{OH})_4$ signatures ($\delta^{30}\text{Si}(\text{OH})_4 \sim +1.2\text{‰}$) as a result

356 of opal remineralisation and the influence of the “production-free” signature of CDW and

357 AABW (Beucher et al., 2008; De La Rocha et al., 2000; de Souza et al., 2012a).

358 ***5.1. Modelling global Si isotope distributions***

359 Modelling of the global marine silicon isotope distribution requires special consideration of

360 deep remineralisation of opal compared to organic matter, and the important role played by
361 the Southern Ocean and, in particular, Mode Waters, which are poorly represented in many
362 climate models. The absolute isotope values obtained in simulations are also sensitive to the
363 $\delta^{30}\text{Si}$ of the Si entering the oceans, although the relative differences between ocean basins and
364 water masses are robust against the isotopic value of the assumed source. Rivers are the main
365 source of Si to the ocean (Tréguer et al. 1995) and have an average $\delta^{30}\text{Si}$ of +0.8‰ (De La
366 Rocha et al., 2000; Georg et al. 2006). The $\delta^{30}\text{Si}$ of river waters is mainly controlled by
367 weathering (Ziegler et al., 2005) and could vary under large climatic or tectonic changes on
368 time scales of 100,000 years or longer (De La Rocha and Bickle, 2005). Hydrothermal waters
369 are another source of Si to the sea (~10% the magnitude of the river source). Few $\delta^{30}\text{Si}(\text{OH})_4$
370 data from hydrothermal fluids are available; two samples collected from vents on the East
371 Pacific Rise show negative values of -0.2 and -0.4‰ close to the average value for igneous
372 rock -0.3‰ (De La Rocha et al., 2000).

373 Wischmeyer et al. (2003) published the first simulation of the global distribution of
374 silicon isotopes in the world ocean using the Hamburg Model of the Ocean Carbon Cycle, V4.
375 This simulation relied on the assumptions that 1) fractionation during silica production is
376 constant with $\epsilon_{\text{DSi-BSi}} = -1.1\text{‰}$, 2) river inputs balance permanent Si burial in sediments and 3)
377 the dissolution of diatom frustules does not affect their isotopic composition (the study was
378 conducted prior to the discovery of fractionation during opal dissolution). Model output
379 showed the $\delta^{30}\text{Si}(\text{OH})_4$ distribution in the surface waters to be inversely related to the
380 $\text{Si}(\text{OH})_4$ concentrations in accordance with the expectation from Rayleigh fractionation of
381 increasing $\delta^{30}\text{Si}(\text{OH})_4$ with greater $\text{Si}(\text{OH})_4$ consumption. Plotting the two variables against
382 each other revealed that their relationship was not a simple Rayleigh distillation curve as the
383 isotopic composition of dissolved silicon not only traces its biological consumption, but also

the mixing of water masses with different $\delta^{30}\text{Si}(\text{OH})_4$ signatures (Wischmeyer et al., 2003). A puzzling result of the Wischmeyer et al. (2003) model was its failure to reproduce the observed decrease in $\delta^{30}\text{Si}(\text{OH})_4$ between the deep Atlantic and Pacific basins (De La Rocha et al 2000), possibly due to an excess of nutrient drawdown in the Southern Ocean due to the lack of iron limitation (Reynolds, 2009).

Multi-box models have been more successful in simulating silicon isotope distributions (De La Rocha and Bickle, 2005; de Souza et al., 2012b; Reynolds, 2009), and new generation GCMs are showing themselves to be promising with respect to reconstructing the Si cycle. Reynolds (2009) used a seven box model (Toggweiler, 1999) and the ten-box PANDORA box model (Broecker and Peng, 1987) to examine global marine silicon isotope distributions. The results of the seven box model are presented here (Figure 4) although the results from the PANDORA model are similar. Incomplete $\text{Si}(\text{OH})_4$ use in the surface waters of the Southern Ocean is a major driver of the model results. The dissolution of diatom frustules formed under incomplete $\text{Si}(\text{OH})_4$ consumption impart similarly light $\delta^{30}\text{Si}(\text{OH})_4$ values to CDW/AABW. The northward flow of Southern Ocean water masses strongly influences the isotopic composition of bottom waters in the Atlantic and Pacific basins. Outside the Southern Ocean the isotopic signature of NADW in the model is largely set by the strong ventilation in the north Atlantic.

5.1.1. Agreement and discrepancies between simulations and measurements

Comparison of the model results of Reynolds (2009) with the few measurements available from the deep Atlantic and Southern Oceans shows both agreement and significant anomalies between model predictions and data. The model predicts the observed relatively heavy $\delta^{30}\text{Si}(\text{OH})_4$ values in NADW and lighter values in CDW (Figure 5). The mechanisms in the model leading to this gradient are the strong biological consumption of $\text{Si}(\text{OH})_4$ in the

408 surface waters feeding into the well ventilated NADW combined with the effects of
409 incomplete Si consumption in Southern Ocean surface waters mentioned above. The model
410 was not constructed in a way to predict $\delta^{30}\text{Si}(\text{OH})_4$ values of the deep waters of the Pacific
411 (Figure 4, 5), but the PANDORA version of the model predicts a decrease in $\delta^{30}\text{Si}(\text{OH})_4$ with
412 increasing $[\text{Si}(\text{OH})_4]$ along the MOC (Reynolds 2009).

413 Beucher et al. (2008)'s examination of the global deep water $\delta^{30}\text{Si}(\text{OH})_4$ data set indicates
414 that key mechanisms are operating in the Pacific that are not captured in current models.
415 When data from waters >2,000 m in the Southern and Pacific Oceans are plotted as a function
416 of $1/[\text{Si}(\text{OH})_4]$ most data fall along a single straight line suggesting that a simple mixing
417 model can explain most results (Figure 5). The high concentration end member is the
418 Northeast Pacific Silicic Acid Plume that originates in the Cascadia Basin (Johnson et al.,
419 2006) that has $[\text{Si}(\text{OH})_4] > 150 \mu\text{M}$ corresponding to a $1/[\text{Si}(\text{OH})_4]$ value of ~ 0.005 in Figure
420 5. The other end member lies in the Southern Ocean. In contrast, the data from the North
421 Pacific and the Northwest Pacific fall on a trajectory of decreasing $\delta^{30}\text{Si}(\text{OH})_4$ with increasing
422 $[\text{Si}(\text{OH})_4]$ from the Atlantic to the Southern Ocean and Pacific as predicted by models
423 (Reynolds 2009).

424 A hypothesis that explains the anomalous isotope patterns in the Pacific is that the Northeast
425 Pacific $\text{Si}(\text{OH})_4$ Plume (Johnson et al. 2006) exerts a major influence on Si isotopes in this
426 region. The flux of $\text{Si}(\text{OH})_4$ from the sediments beneath the Plume is large ($1.5 \text{ Tmol Si a}^{-1}$)
427 equivalent to a third of that supplied to the global ocean by rivers (Johnson et al. 2006). Its
428 influence extends to the west and to the south, but apparently not as far west as the stations in
429 the North Pacific (23°N , 158°W , De La Rocha 2000) and NW Pacific (24.3°N , 170.3°W)
430 presented in Figures 5. This feature has not been incorporated into models of Si isotope
431 distributions. Note that the $\delta^{30}\text{Si}(\text{OH})_4$ of the waters in the Plume, $+1.4\text{‰}$, is much more

positive than hydrothermal sources ($\sim -0.3\%$, De La Rocha et al., 2000) suggesting a biogenic source. The $\delta^{30}\text{Si}(\text{OH})_4$ of the Plume is similar to that in the North Atlantic (Figure 5) so that its influence essentially eliminates contrasts in $\delta^{30}\text{Si}(\text{OH})_4$ between the deep Atlantic and deep Northeast Pacific.

The main point to be taken from this analysis is that the spatial resolution of the present $\delta^{30}\text{Si}(\text{OH})_4$ data set is inadequate to evaluate mechanisms leading to even the first-order distribution of isotopes of Si in the global ocean although strong anomalies point to possible explanations. The level of variability in $\delta^{30}\text{Si}(\text{OH})_4$ within Pacific deep waters far exceeds that predicted by current models and trends between Si isotopes and Si concentration are opposite of model predictions, possibly due the Northeast Pacific Silicic Acid Plume, but other unanticipated mechanisms may be involved. New data from the International GEOTRACES program that is producing sections of $\delta^{30}\text{Si}(\text{OH})_4$ distributions along several major ocean sections should help resolve these issues.

6. Paleoceanographic applications and multi-proxy approaches

In addition to the whole-ocean concentration, biogenic opal production is controlled by the distribution of $\text{Si}(\text{OH})_4$ in the global ocean. Since their evolution, diatoms have dominated the marine silicon cycle and opal formation, such that they have effectively stripped $\text{Si}(\text{OH})_4$ out of surface waters (Falkowski et al., 2004), resulting in pervasive Si limitation of silica production (or co-limitation with other nutrients e.g. iron) in low latitude regions (e.g. Brzezinski et al., 2008; Brzezinski and Nelson, 1996). Net diatom production relies on upwelled sources of dissolved silicon; changes in ocean circulation and upwelling are therefore key to controlling opal production and carbon drawdown by diatoms.

Particular hypotheses that have received attention over the last decade are the Silicic Acid Leakage Hypothesis (SALH; Brzezinski et al., 2002; Matsumoto et al., 2002) and the

related silica hypothesis (Harrison, 2000; Nozaki and Yamamoto, 2001). The silica hypothesis states that diatom productivity was promoted during glacials as a result of an increase in Si supplied from dust, contributing to the drawdown of CO₂ (Harrison, 2000). In contrast, the SALH posits that, during Pleistocene glacials, the addition of iron via enhanced dust deposition in the Southern Ocean results in a change in diatom physiology, such that diatoms take up macronutrients at a lower Si:N ratio. This arises from the combination of decreased cellular N content in most, if not all diatoms, and the thickening or thinning of the siliceous frustules in response to low Fe (Hutchins & Bruland 1998, Takeda, 1998, Marchetti & Harrison 2007). Even in cases where diatoms thin their frustules in response to low Fe (Marchetti & Harisson 2007) the reduction in cellular N is even greater such that increased Si:N is a universal response. The addition of Fe to modern day Southern Ocean waters shifts Si:N uptake ratio from a value of 4-8 under ambient conditions to a value of 2 (Frank et al. 2000). Given the [Si(OH)₄]:[NO₃⁻] ratio of ~2.3 in upwelling waters at the Antarctic Divergence, release from Fe stress during glacial times would cause approximately half of the upwelled silicic acid to remain in surface waters upon nitrate depletion (Brzezinski et al, 2002). The net result is that the water which subducts to form the all-important SOIW that ultimately feed the lower latitude thermocline, would have both higher [Si(OH)₄] and a higher Si:N ratio. Ventilation of the relatively Si-rich SOIW at low latitude would promote the growth of diatoms relative to carbonate producers, altering the C_{org}/CaCO₃ rain ratio and ocean alkalinity to lower atmospheric CO₂ (Matsumoto and Sarmiento, 2008; Rickaby et al., 2007). Opal-based silicon isotope proxies are ideal tools for investigating the SALH, and to investigate other past changes in the marine silicon cycle (Figure 6).

6.1. Silicic acid leakage from the Southern Ocean

6.1.1. Opal mass accumulation rates and ²³¹Pa/²³⁰Th

For the SALH to be accepted, there has to be evidence for a change in Si utilization in the

Southern Ocean, which would have provided the excess Si(OH)_4 to escape to lower latitudes. Records of Southern Ocean opal mass accumulation rates (MAR) since the Last Glacial Maximum (LGM) provide a consensus view that the main belt of opal deposition around Antarctica shifted northwards compared to today, into the subantarctic zone (reviewed by Bradtmiller et al., 2009). These records also imply that there was no net increase in opal production that could have contributed to a drawdown of atmospheric pCO_2 in either the Atlantic or Indian Sectors of the Southern Ocean (Frank et al., 2000; Kumar, 1995). However, there was a decrease during the LGM of total mass flux in the Pacific Sector, which is the main candidate for potential leakage of Si(OH)_4 to the lower latitudes (Bradtmiller et al., 2009; Chase et al., 2003a).

6.1.2. Opal isotope proxies

Si isotope records

Glacial-interglacial changes in Si utilization by diatoms south of the modern Antarctic Polar Front was the first paleoclimate question to be addressed using the diatom opal $\delta^{30}\text{Si}$ proxy (De La Rocha et al., 1998). These first diatom $\delta^{30}\text{Si}$ records showed that there was a lower Si utilization south of the Antarctic Polar Front at the LGM compared to today, and this finding has also been mirrored in sediment cores from the subantarctic (Beucher et al., 2007), supporting the SALH. A reduction in utilization is consistent with a decline in Si uptake by diatoms, relative to other nutrients, as a result of the alleviation of Fe stress. However, changes in dissolution and water column recycling processes, as a result of the alteration of the recirculation that produces the modern silicon trap, could also be responsible for the observed shifts in diatom $\delta^{30}\text{Si}$.

Si-N isotope records

The preferential and variable uptake of Si(OH)_4 over NO_3 in the low-iron waters of the Southern Ocean seawater results in a decoupling of the dynamics of these two

macronutrients and the preferential depletion of $\text{Si}(\text{OH})_4$ over NO_3 in the modern Southern Ocean (Pondaven et al., 2000). The relative utilization of the two nutrients has been constrained over time using combined Si and N isotope records from diatom opal and opal-bound organic matter respectively. One of the principal aims to date has been to investigate changes in Si:N uptake rates in the Southern Ocean over glacial-interglacial timescales as a test of the SALH (Beucher et al., 2007; Crosta et al., 2007; Horn et al., 2011; Robinson et al., 2005b). Although there are analytical challenges surrounding the robust application of diatom-bound N isotopes (Robinson et al., 2004), these studies generally agree that there was relatively higher utilization of N in surface waters compared to $\text{Si}(\text{OH})_4$ during the Last Glacial Maximum, suggesting a relatively high Si:N ratio in Mode Waters, and supporting the SALH (e.g. Horn et al., 2011). More recent studies are beginning to delve into $\text{Si}(\text{OH})_4$ leakage deeper in time, such as an investigation of the role of southern sourced water in driving the highly productive Matuyama Diatom Maximum in the Benguela Upwelling System (Ocean Drilling Program Site 1082, 21.1 °S, 11.8 °E, 1279m water depth) from 2-3 Ma (Etourneau et al., 2012). The heaviest diatom $\delta^{30}\text{Si}$ signal corresponded with the highest opal accumulation rate, and the lightest diatom-bound $\delta^{15}\text{N}$, which could be explained by the growth of mat-forming diatoms due to an increased $\text{Si}(\text{OH})_4$ supply from southern sourced water, but weak upwelling. The mat-forming diatoms efficiently utilised a large proportion of the available Si, resulting in Si-limitation of surface waters and relatively low N utilization (Etourneau et al., 2012).

Paired diatom-sponge Si isotopes

In an analogous fashion to paired benthic-planktonic foraminifera carbon isotopes, paired sponge-diatom silicon isotope records can be used to quantify the marine silicon cycle of the whole water column: the supply of dissolved $\text{Si}(\text{OH})_4$ from deep waters, and the utilization of silicon in surface waters by diatoms in the Southern Ocean. To date, the multi-

proxy approach has been used to investigate the SALH since the Last Glacial Maximum (Hendry et al., 2010; Hendry et al., 2012; Horn et al., 2011). These studies have been able to constrain deep water Si(OH)_4 concentrations (Hendry et al., 2010) and the upwelling rate of Si(OH)_4 (Horn et al., 2011). The records show a dramatic increase in upwelling supply, confirmed an increase in the utilization of Si (Horn et al., 2011), and a slight transient decrease in the concentration of Si(OH)_4 in deep waters across the last glacial termination (Hendry et al., 2010).

Paired Si-Ge records

One important caveat that needs to be considered when reconstructing $[\text{Si(OH)}_4]$ from sponge spicule $\delta^{30}\text{Si}$ using equation 5 is that the isotopic composition of the Si(OH)_4 is required to calculate $\Delta\delta^{30}\text{Si}$. Thus the estimated Si(OH)_4 concentration is a function of the measured spicule $\delta^{30}\text{Si}$ and for paleo - reconstructions, the assumed deep water $\delta^{30}\text{Si(OH)}_4$. As discussed above deep water $\delta^{30}\text{Si(OH)}_4$ is tied to water mass distributions within the MOC in the modern. Deviations from the modern in the past will depend both on i) the secular shift in whole ocean $\delta^{30}\text{Si}$ through time, on timescales greater than the residence time of Si in the global oceans (~10 ka, Georg et al., 2009; Tréguer and De la Rocha, 2013), for example due to changes in subglacial weathering processes and meltwater inputs to the ocean (Opfergelt et al., 2013); and ii) on changes in the distribution of silicon isotopes in the oceans resulting from ocean circulation changes, on timescales of thousands of years or more.

Previous studies have taken these changes into account through simple modelling efforts (e.g. Hendry et al., 2012; Griffiths et al., 2013) or by pairing with diatom $\delta^{30}\text{Si}$ (Egan et al, 2012). However, an alternative approach is to use, in addition to spicule $\delta^{30}\text{Si}$, sponge and diatom Ge/Si ratios. Spicule Ge/Si will record not only secular changes in seawater Ge/Si, which can be corrected for using diatom Ge/Si (thought to be a recorder of secular

changes in whole ocean Ge/Si, although there needs to be a more thorough assessment of vital effects (Froelich et al., 1992), but also a component of Si(OH)₄ concentration. In other words, spicule $\delta^{30}\text{Si}$ and Ge/Si provide complementary access to past ocean Si(OH)₄ concentrations. This approach has been used to investigate the SALH: Ge/Si and Si isotope proxies in sediment cores from the Atlantic and Pacific Sectors (~41°S, ~10°E, 4600m water depth, and ~53°S, ~120°W, 2700m water depth) of the Southern Ocean show that there was a build-up of nutrients during glacial periods in the Pacific Sector only, consistent with opal accumulation records (Bradtmitter et al., 2009; Chase et al., 2003a; Ellwood et al., 2010).

6.2. Impact of silica leakage on the low latitudes

6.2.1. Opal accumulation rates

Records of opal mean accumulation rate (MAR), ^{230}Th -normalised opal MAR, and downcore $^{231}\text{Pa}/^{230}\text{Th}$ do not reveal a clear picture of changes in low latitude diatom productivity over glacial-interglacial and millennial timescales in response to Si(OH)₄ leakage, pointing towards multiple controls in Si supply and uptake. In the Central and Eastern Equatorial Pacific, and the Peru upwelling zone, ^{230}Th -normalised opal fluxes are higher at Marine Isotope Stage (MIS) 3 (~30-60 ka) than during MIS2 (~20-30 ka), with either similar or lower opal fluxes during the Last Glacial Maximum compared to the Holocene, which is inconsistent with the SALH (Bradtmitter et al., 2006; Kienast et al., 2006; Richaud et al., 2007). However, records going back further into the Pleistocene show higher ^{230}Th -normalised opal fluxes at the glacial terminations than at full glacial conditions or during interglacials, but these peaks are not observed for all terminations, and there are peaks in opal flux not associated with terminations (Bradtmitter et al., 2006; Dubois et al., 2010; Hayes et al., 2011). In contrast, the Eastern Tropical North Pacific (ETNP) shows higher opal MAR at the glacials compared to the interglacials (Arellano-Torres et al., 2011). In the Western Pacific, large diatom mats in the Phillipines Sea, comprising *Ethmodiscus rex*, have

been carbon dated to MIS2 (Zhai et al., 2009). However, $^{231}\text{Pa}/^{230}\text{Th}$ and ^{230}Th -normalised opal fluxes from another core in the Western Equatorial Pacific indicates lower productivity in glacial periods (Pichat et al., 2004).

Similar inconsistencies occur in the Atlantic. In the Equatorial Atlantic, the sediment cores that have been analyzed to date show higher opal accumulation and corresponding $^{231}\text{Pa}/^{230}\text{Th}$ during the last glacial, with peaks occurring at the deglaciation, although these cores do not have sufficient sedimentation rates to resolve fully Heinrich Stadials, the abrupt climate events of the late glacial and deglacial (Bradtmeier et al., 2007). Other sites in the Eastern North Atlantic show clearer abrupt increases in opal export during the deglacial, which correspond with oceanic and/or atmospheric reorganisation during the Heinrich Stadials (Meckler et al., 2013; Romero et al., 2008).

In addition to inherent preservation bias, there are a number of reasons why the low latitude opal accumulation rate records need to be treated carefully in the context of the SALH. Firstly, the opal MAR records reveal complex temporal and spatial patterns, reflecting a number of regional and local controls on productivity. Secondly, tropical opal burial reconstructions cannot distinguish between the silica hypothesis of Harrison (2000) and the SALH *sensu stricto* (Brzezinski et al., 2002) i.e. opal records cannot provide a mechanistic interpretation for productivity changes. Thirdly, $\text{Si}(\text{OH})_4$ leakage may not manifest in an increase in opal accumulation rate, *per se*, but an increase in the productivity of opal-producers relative to carbonate producers, and still produce a shift in ocean alkalinity and pCO_2 drawdown (Matsumoto & Sarmiento, 2008). In other words, the lack of a coherent change in low latitude opal accumulation rates is not sufficient to reject the SALH. Instead, a multi-proxy approach allows the various interacting controls on productivity to be deconvolved, and specific hypotheses regarding the SALH to be tested.

6.2.2. Multi-proxy isotope records of low latitude changes in water mass and ecology

605 *Sponge spicule silicon isotopes*

606 An important concept that follows from the SALH is that intermediate waters
607 subducting away from the Southern Ocean must have increased in Si(OH)_4 during the glacial.
608 Sponge spicule $\delta^{30}\text{Si}$ records of benthic Si(OH)_4 concentrations provides one of the most
609 direct methods for testing this assertion. Spicule isotopic records from core site GeoB2107-3
610 (27°S, 46°W, 1050 m water depth), which is bathed in modern AAIW, show that the Si(OH)_4
611 concentrations were not significantly different at the LGM compared to today. However, the
612 records show pulses of heavy $\delta^{30}\text{Si}$ – indicative of high Si(OH)_4 concentrations – during the
613 abrupt events of the late glacial and deglacial, Heinrich Stadials (HS) One and Two, and the
614 Younger Dryas (Hendry et al., 2012). In other words, leakage of high Si waters from the
615 Southern Ocean to lower latitudes occurs, but during abrupt climate change events rather than
616 on glacial-interglacial timescales.

617 *Paired Si-Nd isotopes*

618 Due to biogeographical variations and ocean circulation, Southern Ocean deep waters
619 are characteristically Si(OH)_4 -rich, and changes in their Si(OH)_4 content can be traced by the
620 $\delta^{30}\text{Si}$ of benthic sponge spicules (Hendry et al., 2010). The Nd isotope composition (ϵNd) of
621 bottom water, recorded in fish teeth, sediments, and Fe-Mn coatings of planktonic
622 foraminifera in some oceanographic settings (e.g. Pahnke et al., 2008; Piotrowski et al., 2008;
623 Roberts et al., 2010), provides an additional method of “labelling” southern sourced waters,
624 due to a distinctive radiogenic signature from mixing with Pacific waters (Albarede et al.,
625 1997). However, one key problem with the ϵNd proxy is that the Nd southern and northern
626 end members could change over relevant timescales (Pahnke et al., 2008). The part of the
627 water column that is represented by planktonic foraminiferal coatings is also apparently
628 variable (Pena et al., 2013; Roberts et al., 2010). A combination of these benthic $\delta^{30}\text{Si}$ and

εNd can, however, provide a more robust means of tracing southern sourced water.

To date, this has been used to investigate the SALH across MIS4 (~60-70 ka) in the tropical Atlantic (Griffiths et al., 2013), and more localised processes in the Peruvian upwelling zone of the South Pacific (Ehlert et al., 2013). Of relevance to the SALH, Griffiths et al. (2013) found that both “tracers” indicated an increase in the presence of southern component water in a sediment core off the coast of Brazil (core site MD99-2198, 12.09°N; 61.23°W; 1330m water depth) across the MIS 5/4 boundary, consistent with a modest leakage of relatively Si-enriched water from the Southern Ocean at this time via SOIW. However, further work is required to understand the relationship between these two proxies, given the slight differences in the timing and nature of the changes recorded in core MD99-2198.

Si-N isotopes

Diatom Si and diatom-bound N isotopes from a core in the Eastern Equatorial Pacific support a reduction in Si uptake relative to other nutrients due to the alleviation of Fe stress – and limitation by Si and N - during the glacial. The authors argue for a fundamental change in nutrient limitation in the region, with a likely glacial switch to phosphorus limitation away from Si-Fe co-limitation (Pichevin et al., 2009).

7. Silicic Acid Leakage form the Southern Ocean – New Insights and Changing Perspectives

The SALH has been tested repeatedly over the past few years. One of the key issues, and the main defining difference between the silica hypothesis (Harrison , 2000) and the SALH *senso stricto* (Brzezinski et al., 2002), is the extent to which SOIW distributions have changed over glacial-interglacial and millennial timescales. Other geochemical archives have been used to investigate changes in intermediate water formation and distribution, including stable carbon isotopes (Spero and Lea, 2002; Bostock et al., 2004; Pahnke & Zahn, 2005; Bostock et al., 2010), diatom-bound carbon isotopes (Xiong et al., 2013), radiocarbon (Burke

and Robinson, 2011; Keigwin, 2004; Mangini et al., 2010; Robinson et al., 2005a; Thornalley et al., 2011), ϵNd (Pahnke et al., 2008; Pena et al., 2013; Xie et al., 2012), and biomarkers (Calvo et al., 2004; Calvo et al., 2011; dos Santos et al., 2012; Higginson and Altabet, 2004). Some coherent pictures have begun to arise of expanded AAIW during glacials, especially in the Pacific (Bostock et al., 2004, 2010), with intense deep mixing with CDW and Glacial Antarctic Bottom Water (GAABW), expanded oligotrophic surface waters in the Subantarctic and so a strong subsurface nutrient gradient (Bostock et al., 2004, 2010). Furthermore, carbon isotopes suggest widespread pulses of well-ventilated SOIW formation during the Heinrich Stadials and Younger Dryas (Pahnke & Zahn, 2005).

Other lines of evidence point towards expanded SOIW during abrupt climate events of the deglacial e.g. Nd isotope record from the Tobago Basin and East Equatorial Pacific (Pahnke et al., 2008; Pena et al., 2013). Another ϵNd record from the Florida Straits points towards reduced SOIW presence in the North Atlantic during Heinrich Stadial One and the Younger Dryas (Xie et al., 2012). However, this study assumed almost pure AAIW filled the study site basin, an assumption that is not supported by modern hydrographic data (Pena et al., 2013). These disagreements highlight the complex nature of reconstructing oceanic circulation, and the problems with geochemical proxies, for example in terms of signal redistribution (Gutjahr et al., 2008) and changing water mass end-members (Pahnke et al., 2008).

The opal-based evidence from the Southern Ocean discussed above, combining opal $\delta^{30}\text{Si}$ records with other palaeoproxies, indicates that there were major ecological changes in the Southern Ocean over glacial-interglacial timescales, which would have led to a change in the composition of SOIW. The Si:N ratio would increase during glacials either due to a change in i) utilization of Si relative to N as a result of Fe fertilization (Brzezinski et al., 2002), or ii) the location of the opal belt such that dissolution and regeneration of opal occurs

in the region of SOIW subduction (Bradtmitter et al., 2007). However, proxy evidence from low latitudes suggests that, on glacial-interglacial timescales, the impact on lower latitude ecology, and climate, was minimal. A reduction in the rate of SOIW supply, or indeed a change in the depths to which the subducted waters penetrated, over glacial-interglacial timescales may have limited the extent to which the southern sourced preformed nutrients could upwell in the low latitudes (Crosta et al., 2007). Rather, it was changes on abrupt (millennial) timescales in ocean circulation and wind-driven upwelling (Anderson et al., 2009; Moreno et al., 2002) during glacial terminations that enhanced the supply of – most likely – southern sourced Si-rich water that drove the major ecological changes observed in lower latitude sedimentary cores (Pahnke et al., 2008; Hendry et al., 2012; Calvo et al., 2011; Bradtmiller et al., 2008). The most-cited sources for these southern-component waters are SOIW (e.g. Pahnke et al., 2008; Calvo et al., 2011; Pena et al., 2012; Hendry et al., 2012), which are known to feed the lower thermocline with nutrients in the low latitudes (Sarmiento et al., 2004). However, it has also been speculated that the Si(OH)_4 feeding the low latitude peaks in opal production seen in the Equatorial and North Atlantic originated from upwelling deep southern component water through a large-scale change in ocean circulation (Meckler et al., 2013). However, the similarity of the deglacial opal peaks in the low-latitude Atlantic and Pacific Oceans (Bradtmitter et al., 2006, 2007) would require a process that could operate in both basins despite the different deep-water mass configurations, and so could be used to argue against a deep southern component water mechanism.

Could changing nutrient dynamics in the Southern Ocean alter southern-sourced Mode Waters to cause major changes in nutrient distribution during abrupt climate change? Whilst a speculative twist on the SALH, such events may be the logical outcome of the shifts in Southern Ocean circulation and nutrient supply during glacial terminations. Glacial periods are characterized by the northward shift in the westerly winds in the Antarctic coupled

704 with strong stratification south of the Polar Front due to buoyancy-forcing and reduced wind-
705 stress (Marshall & Speer, 2012). Diatom productivity and the opal belt also shifted northward
706 supported mainly by upwelling within the Subantarctic (Beucher et al., 2007, Bostock et al.,
707 2004). Upwelling and mixing to the north of the Polar Front in the Subantarctic would not be
708 as efficient in tapping high-nutrient deeper waters compared to the circulation associated with
709 the Antarctic Divergence, diminishing nutrient supply during glacials. The northward shift in
710 the opal belt may have been coupled with a reduction in residual silicic acid concentrations as
711 a result of a lower supply of Si to the Subantarctic surface waters and significant diatom
712 production. Combined with high atmospheric Fe supply this would result in SOIW with high
713 Si:N ratio, but diminished Si concentrations. Hence, SOIW mixing with low-latitude
714 thermocline waters did not promote significant diatom growth, especially in regions where
715 wind-driven upwelling was also weakened during glacial times (e.g. Moreno et al., 2002).
716 However, during HS1, sustained Fe supply to the Southern Ocean, continued mixing in the
717 Subantarctic (e.g. Bostock et al., 2004), together with a breakdown of stratification and
718 increased upwelling in the Antarctic (e.g. Anderson et al., 2009; Burke & Robinson, 2011)
719 would re-establish the Antarctic Divergence and - once again – lead to the efficient tapping of
720 deeper waters. Such an increase in upwelling would result in an increase in both Si and
721 oceanic Fe supply to surface waters (Ayers & Strutton, 2013), despite reducing atmospheric
722 Fe input (Lambert et al., 2008). Strong wind-driven mixing would result in deep winter
723 convection (Holte et al., 2012) and formation of SOIW with high Si concentrations and high
724 Si:N. At the same time, enhanced wind-driven upwelling in the lower latitudes increased the
725 supply of these waters to the thermocline and so supported enhanced diatom growth. Whilst
726 the atmospheric Fe supply to the surface of the Southern Ocean had declined by the Younger
727 Dryas (Lambert et al., 2008), and the Southern Ocean Si trap was re-established, low-latitude
728 diatom pulses still occurred in places of enhanced wind-driven upwelling as a response to

enhanced mixing of oceanic Fe in the Subantarctic and changes in the vertical structure of SOIW (Hendry et al., 2012).

Key to this scenario is the change in the efficiency with which Southern Ocean circulation brings abyssal waters with high nutrients to the surface where opal formation occurs. During the glacials, that efficiency is low due to increased stratification and reduced mixing in Antarctic waters coupled with the northwards shift in the opal belt from the Antarctic Divergence to the Subantarctic, where entrainment of high-nutrient abyssal water is less pronounced. A southwards shift in the opal belt and enhanced upwelling and mixing in the Antarctic Divergence during Heinrich Stadials would increase the efficiency of oceanic nutrient supply from deep waters, and both the Si content and Si:N ratio of mode waters (Ayers & Strutton, 2013). Together these factors form the basis of a **“Silicic Acid Ventilation Hypothesis” (SAVH)** (Figure 7) where the change in oceanic and atmospheric circulation that occurred during the Heinrich Stadials would lead both to the ventilation of waters near the Antarctic Divergence, resulting in Si-enriched SOIW, and the low-latitudes, leading to the supply of these high Si waters to the surface and triggering the widespread and abrupt ecological changes that are observed. Further investigation into intermediate depth water composition, using high-resolution records of diatom and spicule $\delta^{30}\text{Si}$, in addition to the other proxies discussed above, will be able to test the plausibility of such a mechanism.

The original SALH proposed that Si leakage during glacial times contributed to global cooling by lowering atmospheric pCO_2 during glacial periods. The more recent evidence that Si leakage from the Southern Ocean occurred predominately during deglaciations has profound implications for the effect of this mechanism on climate. Si leakage during deglaciations would drive low latitude flora towards diatoms when atmospheric pCO_2 levels were rising. This suggests that the ecological effects that would favour a decline in atmospheric pCO_2 was overwhelmed by other, possibly physical processes, such as the

754 increased evasion of CO₂ from the ocean due to increased upwelling at the Antarctic
755 Divergence (Anderson et al 2009).

756 **8.Synthesis and Conclusions**

757 The Southern Ocean plays a key role in the climate system, through heat and nutrient
758 transfer to the global oceans. The “biogeochemical divide” formed by the Antarctic
759 Divergence, and the formation of Mode Waters, essentially sets the global levels of preformed
760 nutrients and stored carbon (Marinov et al., 2008; Marinov et al., 2006; Sarmiento et al.,
761 2004; Sigman et al., 2010). Understanding Mode Water nutrients, and how they have
762 changed in the past, is essential for understanding past changes in both Southern Ocean and
763 low latitude biological productivity. Diatoms dominate the phytoplankton communities in
764 most regions of the Southern Ocean, and they impart distinctive Si(OH)₄ concentrations and
765 isotope signatures on the subducting waters that form the Mode Waters. The established
766 relationship between isotopes of Si and the MOC allows the proxy to be used as both a
767 nutrient proxy and an indicator of water mass changes. Furthermore, biogenic opal provides
768 an important archive of past ocean biological productivity and environmental conditions in
769 the Southern Ocean and beyond. In particular, when used in conjunction with other
770 sedimentary proxies, biogenic opal $\delta^{30}\text{Si}$ has shown itself to have great potential in
771 deconvolving past signals of climatic, biogeochemical and ecological change.

772 **Acknowledgements**

773 KH is funded by the Royal Society, the Climate Change Consortium of Wales, the Natural
774 Environment Research Council, and the Leverhulme Trust. MB is funded by the US National
775 Science Foundation.

776 Figure 1:

777 Schematic of the transport of $\text{Si}(\text{OH})_4$ in the ocean and the relationship with the MOC, after

778 Marinov et al. (2008). The double-headed arrows show the major water masses, shaded

779 according to $\text{Si}(\text{OH})_4$ concentration. The dashed line shows the thermocline depth.

780 Figure 2:

781 Apparent fractionation factors estimated from a number of culture, water column and

782 sediment core top studies. (Beucher et al., 2008; Cao et al., 2012; Cardinal et al., 2005; De

783 La Rocha et al., 1997; De La Rocha et al., 2011; Egan et al., 2012; Ehlert et al., 2013; Fripiat

784 et al., 2012; Fripiat et al., 2011; Milligan et al., 2004; Reynolds et al., 2006; Sutton et al.,

785 2013; Varela et al., 2004).

786 Figure 3:

787 $\Delta\delta^{30}\text{Si}$ for all sponges from different ocean basins. The modern sponges (open symbols) were

788 measured without Mg doping, with error bars showing 2SD ($\sim\pm 0.2\text{‰}$ for $\delta^{30}\text{Si}$ and 0.4‰

789 for $\Delta\delta^{30}\text{Si}$). The core-top spicules (solid symbols) were measured with Mg doping, with error

790 bars showing 2SD ($\sim\pm 0.1\text{‰}$ for $\delta^{30}\text{Si}$). Unless specified, data are from Hendry & Robinson,

791 2012.

792 Figure 4:

793 Results using a seven box model simulating $\text{Si}(\text{OH})_4$ concentrations and $\delta^{30}\text{Si}(\text{OH})_4$

794 distributions (*italics in parentheses*). Surface boxes from left to right correspond to the

795 Antarctic, Subantarctic, Low Latitude surface waters and the Subarctic. Adapted from

796 Reynolds (2009). Abbreviations taken from Reynolds (2009): AAIW = Antarctic

797 Intermediate Water (essentially Mode Waters comprising Antarctic Intermediate Waters and

798 Subantarctic Mode Water); CDW = Circumpolar Deep Water; NADW = North Atlantic Deep

799 Water.

800 Figure 5:

801 $\delta^{30}\text{Si}$ versus $1/[\text{Si}(\text{OH})_4]$ for waters below 2000 m (adapted from Beucher et al., 2008). EEP,
802 Eastern equatorial Pacific; AZ, Antarctic Zone; SAZ, Subantarctic Zone; PFZ, Polar Frontal
803 Zone; HOTS, Hawaiian Oceanic Time Series; BaTS, Bermuda Time Series. Linear regression
804 of data from Southern Ocean and Eastern Pacific. Gray line drawn by eye. Model results
805 from Reynolds (2009).

806 Figure 6:

807 Map showing location of studies specifically aimed at investigating the SALH. Drawn using
808 Ocean Data View. (Arellano-Torres et al., 2011; Beucher et al., 2007; Bradtmiller et al.,
809 2006, 2007, 2009; Calvo et al., 2004; Calvo et al., 2011; Chase et al., 2003a; Crosta et al.,
810 2007; De La Rocha et al., 1998; dos Santos et al., 2012; Dubois et al., 2010; Ehlert et al.,
811 2013; Ellwood et al., 2010; Frank et al., 2000; Hayes et al., 2011; Hendry et al., 2010; Hendry
812 et al., in revision; Hendry et al., 2012; Higginson and Altabet, 2004; Horn et al., 2011;
813 Kienast et al., 2006; Kumar, 1995; Meckler et al., 2013; Pena et al., 2013; Pichat et al., 2004;
814 Pichevin et al., 2010; Pichevin et al., 2009; Richaud et al., 2007; Robinson et al., 2005b;
815 Romero, 2010; Romero et al., 2011; Zhai et al., 2009)

816 Figure 7:

817 Cartoon illustrating the “**Silicic Acid Ventilation Hypothesis**” (SAVH). LCDW = Lower
818 Circumpolar Deep Water; GNAIW = Glacial North Atlantic Intermediate Water; GAABW =
819 Glacial Antarctic Bottom Water; SOIW = Southern Ocean Intermediate Water. The black
820 triangle shows the location of the Southern Ocean opal belt.
821 During the LGM, Mode Waters formed with a high Si:N ratio, due to changes in utilization
822 and dissolution processes resulting from Fe fertilization and a northwards movement of the
823 opal belt (Bradtmiller et al., 2009). Buoyancy-driven stratification in the Southern Ocean and

824 weaker mixing in the Subantarctic , coupled with weaker upwelling in key regions (e.g.
825 Benguela Upwelling System, (Romero, 2010)) increases the ratio of Si:N in SOIW, but
826 reduces the concentration of Si, and so reduces the supply of Si to low-latitude thermocline
827 waters.

828 At Heinrich Stadial 1 (HS1, 16-18 ka), ice-rafting in the North Atlantic drives a collapse of
829 GNAIW (McManus et al., 2004), a southwards shift of the Atlantic Intertropical Convergence
830 Zone (ITCZ), a strengthening of the NE Trade Winds (Vink et al., 2001) and a southwards
831 shift in the Southern Ocean Westerlies (Anderson et al., 2009). These atmospheric changes
832 could have resulted in stronger upwelling in some regions of the North Atlantic and Pacific
833 Oceans (Koutavas and Sachs, 2008; McClymont et al., 2012). Enhanced wind-driven
834 upwelling, and greater mixing in the Subantarctic, together with a breakdown of buoyancy-
835 driven stratification in the Southern Ocean, would have led to high Si:N and high Si
836 concentration SOIW. A concurrent increase in ventilation in the Southern Ocean and the low-
837 latitudes would have led both to an export of these high Si:N and high [Si] waters and an
838 increase in their supply to thermocline and surface waters, promoting low-latitude diatom
839 production.

- Albarede, F., Goldstein, S. L., Dautel, D., 1997, The neodymium isotopic composition of manganese nodules from the Southern and Indian Oceans, the global oceanic neodymium budget, and their bearing on deep ocean circulation. *Geochimica et Cosmochimica Acta* 61 (6), 1277-1291.
- Andersen, M. B., Vance, D., Archer, C., Anderson, R. F., Ellwood, M. J., Allen, C. S., 2011, The Zn abundance and isotopic composition of diatom frustules, a proxy for Zn availability in ocean surface seawater. *Earth and Planetary Science Letters* 301, 137-145.
- Anderson, R. F., Ali, S., Bradtmiller, L. I., Nielsen, S. H. H., Fleisher, M. Q., Anderson, B. E., Burckle, L. H., 2009, Wind-driven upwelling in the Southern Ocean and the deglacial rise in atmospheric CO₂. *Science* 323, 1443-1448.
- Arellano-Torres, E., Pichevin, L. E., Ganeshram, R. S., 2011, High-resolution opal records from the eastern tropical Pacific provide evidence for silicic acid leakage from HNLC regions during glacial periods. *Quaternary Science Reviews* 30, (9-10), 1112-1121.
- Ayers, J.M., Strutton, P.G., 2013, Nutrient variability in Subantarctic Mode Waters forced by the Southern Annular Mode and ENSO. *Geophysical Research Letters*, 40, 3419–3423,
- Beucher, C. P., Brzezinski, M. A., Crosta, X., 2007, Silicic acid dynamics in the glacial sub-Antarctic: Implications for the silicic acid leakage hypothesis. *Global Biogeochemical Cycles* 21, doi:10.1029/2006GB002746.
- Beucher, C. P., Brzezinski, M. A., Jones, J. L., 2008, Sources and biological fractionation of silicon isotopes in the Eastern Equatorial Pacific. *Geochimica et Cosmochimica Acta* 72, 3063-3073.
- Bostock, H.C., Opdyke, B.N., Gagan, M.K., Fitfield, L.K., 2004, Carbon isotope evidence for changes in Antarctic Intermediate Water circulation and ocean ventilation in the southwest Pacific during the last deglaciation. *Paleoceanography* 19, doi:10.1029/2004PA001047.
- Bostock, H.C., Opdyke, B.N. Williams, M.J.M., 2010, Characterising the intermediate depth waters of the Pacific Ocean using $\delta^{13}\text{C}$ and other geochemical tracers: Deep Sea Research Part 1: Oceanographic Research Papers 57 (7), 847-859.
- Bradtmiller, L. I., Anderson, R. F., Fleisher, M. Q., Burckle, L. H., 2006, Diatom productivity in the equatorial Pacific Ocean from the last glacial period to the present: a test of the silicic acid leakage hypothesis. *Paleoceanography* 21, doi: 10.1029/2006PA001282.
- , 2007, Opal burial in the equatorial Atlantic Ocean over the last 30 ka: implications for glacial-interglacial changes in the ocean silicon cycle. *Paleoceanography* 22, doi:10.1029/2007PA001443.
- , 2009, Comparing glacial and Holocene opal fluxes in the Pacific sector of the Southern Ocean. *Paleoceanography* 24, doi:10.1029/2008PA001693.
- Broecker, W. S., Peng, T.-H., 1987, The role of CaCO₃ compensation in the glacial to interglacial atmospheric CO₂ change. *Global Biogeochemical Cycles* 1, 15-29.
- Brzezinski, M. A., Dumoussaud, C., Krause, J. W., Measures, C. I., Nelson, D. M., 2008, Iron and silicic acid concentrations together regulate Si uptake in the equatorial Pacific Ocean. *Limnology and Oceanography* 53, 875-889.
- Brzezinski, M. A., Nelson, D. M., 1996, Chronic substrate limitation of silicic acid uptake rates in the western Sargasso Sea. *Deep-Sea Research II* 43, 437-453.
- Brzezinski, M. A., Sigman, D. M., Sarmiento, J. L., Matsumoto, K., Gruber, N., Rau, G. H., Coale, K. H., 2002, A switch from Si(OH)₄ to NO₃⁻ depletion in the glacial Southern Ocean. *Geophysical Research Letters*, 29, 1564.
- Burke, A., Robinson, L. F., 2011, The Southern Ocean's role in carbon exchange during the

last deglaciation. *Science* 335 (6068), 557-561.

Calvo, E., Pelejaro, C., Logan, G. A., Deckker, P., 2004, Dust-induced changes in phytoplankton composition in the Tasman Sea during the last four interglacials. *Paleoceanography* 19, PA2020.

Calvo, E., Pelejero, C., Pena, L. D., Cacho, I., Logan, G. A., 2011, Eastern Equatorial Pacific productivity and related-CO₂ changes since the last glacial period. *Proceedings of the National Academy of Sciences of the USA* 108, 5537-5541.

Cao, Z., Frank, M., Dai, M., Grasse, P., Ehlert, C., 2012, Silicon isotope constraints on sources and utilization of silicic acid in the northern South China Sea. *Geochimica et Cosmochimica Acta* 97, 88-104.

Cardinal, D., Alleman, L. Y., Dehairs, F., Savoye, N., Trull, T. W., Andre, L., 2005, Relevance of silicon isotopes to Si-nutrient utilization and Si-source assessment in Antarctic waters. *Global Biogeochemical Cycles* 19, doi:10.1029/2004GB002364.

Cardinal, D., Savoye, N., Trull, T. W., Dehairs, F., E.E., K., Fripiat, F., Tison, J.-L., André, L., 2007, Silicon isotope in spring Southern Ocean diatoms: large zonal changes despite homogeneity among size fractions. *Marine Chemistry* 106, 46-62.

Chase, Z., Anderson, R. F., Fleisher, M. Q., Kubik, P. W., 2002, The influence of particle composition and particle flux on the scavenging of Th, Pa and Be in the ocean. *Earth and Planetary Science Letters* 204, 215-229.

-, 2003a, Accumulation of biogenic and lithogenic material in the Pacific sector of the Southern Ocean during the past 40,000 years. *Deep-Sea Research II* 50, 799-832.

-, 2003b, Scavenging of Th-230, Pa-231 and Be-10 in the Southern Ocean (SW Pacific Sector): the importance of particle flux, particle composition and advection. *Deep-Sea Research II: Topical Studies in Oceanography* 50, 739-768.

Cortese, G., Gersonde, R., Hillenbrand, C.-D., Kuhn, G., 2004, Opal sedimentation shifts in the World Ocean over the last 15 Myr. *Earth and Planetary Science Letters* 224, 509-527.

Crosta, X., Beucher, C., Pahnke, K., Brzezinski, M. A., 2007, Silicic acid leakage from the Southern Ocean: opposing effects of nutrient uptake and oceanic circulation. *Geophysical Research Letters* 34, L13601, doi:10.1029/2006GL029083.

De La Rocha, C., Bickle, M., 2005, Sensitivity of silicon isotopes to whole-ocean changes in the silica cycle. *Marine Geology* 217, 267-282.

De La Rocha, C., Brzezinski, M. A., DeNiro, M. J., 1997, Fractionation of silicon isotopes by marine diatoms during biogenic silica formation. *Geochimica Cosmochimica Acta* 61, 5051-5056.

De La Rocha, C., Brzezinski, M. A., DeNiro, M. J., Shemesh, A., 1998, Silicon isotope composition of diatoms as an indicator of past oceanic change. *Nature* 395, 680-683.

De La Rocha, C. L., 2003, Silicon isotope fractionation by marine sponges and the reconstruction of the silicon isotope composition of ancient deep water. *Geology* 31, 423-426.

De La Rocha, C. L., Bescont, P., Croguennoc, A., Ponzevera, E., 2011, The silicon isotope composition of surface waters in the Atlantic and Indian Sectors of the Southern Ocean. *Geochimica et Cosmochimica Acta* 75 (18), 5283-5295.

De La Rocha, C. L., Brzezinski, M. A., DeNiro, M. J., 2000, A first look at the distribution of the stable isotopes of silicon in natural waters. *Geochimica et Cosmochimica Acta* 64, 2467-2477.

de Souza, G. F., Reynolds, B. C., Johnson, G. C., Bullister, J. L., Bourdon, B., 2012a, Silicon stable isotope distribution traces Southern Ocean export of Si to the eastern South Pacific thermocline. *Biogeosciences* 9, 4199-4213.

938 de Souza, G. F., Reynolds, B. C., Rickli, J., Frank, M., Saito, M. A., Gerringa, L. J. A.,
 939 Bourdon, B., 2012b, Southern Ocean control of silicon stable isotope distribution in
 940 the deep Atlantic Ocean. *Global Biogeochemical Cycles* 26 (2),
 941 doi:10.1029/2011GB004141.
 942 Demarest, M. S., Brzezinski, M. A., Beucher, C., 2009, Fractionation of silicon isotopes
 943 during biogenic silica dissolution. *Geochimica et Cosmochimica Acta* 73, 5572-5583.
 944 DeMaster, D. J., 2002, The accumulation and cycling of biogenic silica in the Southern
 945 Ocean: revisiting the marine silica budget. *Deep-Sea Research II* 49, 3155-3167.
 946 dos Santos, R. A. L., Wilkins, D., De Deckker, P., Schouten, S., 2012, Late Quaternary
 947 productivity changes from offshore Southeastern Australia: A biomarker approach.
 948 *Palaeogeography Palaeoclimatology Palaeoecology* 363, 48-56.
 949 Dubois, N., Kienast, M., Kienast, S., Calvert, S. E., Francois, R., Anderson, R. F., 2010,
 950 Sedimentary opal records in the eastern equatorial Pacific: it's not all about leakage.
 951 *Global Biogeochemical Cycles* 24, GB4020, doi:10.1029/2010GC003821.
 952 Egan, K., Rickaby, R. E. M., Leng, M. J., Hendry, K. R., Hermoso, M., Sloane, H. J.,
 953 Bostock, H., Halliday, A. N., 2012, Diatom silicon isotopes as a proxy for silicic acid
 954 utilisation: A Southern Ocean core top calibration. *Geochimica et Cosmochimica Acta*
 955 96, 174-192.
 956 Ehlert, C., Grasse, P., Frank, M., 2013, Changes in silicate utilisation and upwelling intensity
 957 off Peru since the Last Glacial Maximum - insights from silicon and beryllium
 958 isotopes. *Quaternary Science Reviews* 72, 18-35.
 959 Ellwood, M. J., Hunter, K. A., 1999, Determination of the Zn/Si ratio in diatom opal: a
 960 method for the separation, cleaning and dissolution of diatoms. *Marine Chemistry* 66,
 961 149-160.
 962 Ellwood, M. J., Wille, M., Maher, W., 2010, Glacial silicic acid concentrations in the
 963 Southern Ocean. *Science* 330, 1088-1091.
 964 Etourneau, J., Ehlert, C., Frank, M., Martinez, P., Schneider, R., 2012, Contribution of
 965 changes in opal productivity and nutrient distribution in the coastal upwelling systems
 966 to Late Pliocene/Early Pleistocene climate cooling. *Climate of the Past* 8, 1435-1445.
 967 Falkowski, P. G., Katz, M. E., Knoll, A. H., Quigg, A., Raven, J. A., Schofield, O., Taylor, F.
 968 J. R., 2004, The evolution of modern eukaryotic phytoplankton. *Science* 305, 354-
 969 360.
 970 Frank, N., Gersonde, R., Rutgers van der Loeff, M. M., Bohrmann, G., Nürnberg, C. C.,
 971 Kubik, P. W., Suter, M., Mangini, A., 2000, Similar glacial and interglacial export
 972 productivity in the Atlantic sector of the Southern Ocean. Multiproxy evidence and
 973 implications for glacial atmospheric CO₂. *Paleoceanography* 15, 642-658.
 974 Fripiat, F., Cardinal, D., Tison, J.-L., Worby, A., André, L., 2007, Diatom-induced silicon
 975 isotopic fractionation in Antarctic sea ice. *Journal of Geophysical Research* 112,
 976 doi:10.1029/2006JG000244.
 977 Fripiat, F., Cavagna, A.-J., Dehairs, F., de Brauwere, A., Andre, L., Cardinal, D., 2012,
 978 Processes controlling the Si-isotopic composition in the Southern Ocean and
 979 application for paleoceanography. *Biogeosciences* 9, 2443-2457.
 980 Fripiat, F., Cavagna, A.-J., Savoye, N., Dehairs, F., Andre, L., Cardinal, D., 2011, Isotopic
 981 constraints on the Si-biogeochemical cycle of the Antarctic Zone in the Kerguelen area
 982 (KEOPS). *Marine Chemistry* 123 (1-4), 11-22.
 983 Froelich, P. N., Blanc, V., Mortlock, R. A., Chillrud, S. N., 1992, River fluxes of dissolved
 984 silica to the ocean were higher during glacials. *Ge/Si in diatoms, rivers and oceans:*
 985 *Paleoceanography* 7, 739-767.
 986 Georg, R. B., West, A. J., Basu, A. R., Halliday, A. N., 2009, Silicon fluxes and isotope

987 composition of direct groundwater discharge into the Bay of Bengal and the effect on
 988 the global ocean silicon budget. *Earth and Planetary Science Letters* 283 (1-4), 67-74.
 989 Griffiths, J. D., Barker, S., Hendry, K. R., Thornalley, D. J. R., van de Flierdt, T., Hall, I. R.,
 990 Anderson, R. F., 2013, Evidence of silicic acid leakage to the tropical Atlantic via
 991 Antarctic Intermediate Water during marine isotope stage 4. *Paleoceanography* 28,
 992 307-318.
 993 Gutjahr, M., Frank, M., Stirling, C. H., Keigwin, L. D., Halliday, A. N., 2008, Tracing the Nd
 994 isotope evolution of North Atlantic deep and intermediate waters in the western North
 995 Atlantic since the Last Glacial Maximum from Blake Ridge sediments: *Earth and*
 996 *Planetary Science Letters* 266 (1-2), 61-77.
 997 Harrison, K. G., 2000, Role of increased marine silica input on paleo-pCO₂ levels.
 998 *Paleoceanography* 15, 292-298.
 999 Hayes, C. T., Anderson, R. F., Fleisher, M. Q., 2011, Opal accumulation rates in the equatorial
 1000 Pacific and mechanisms of deglaciation. *Paleoceanography* 26, PA1207,
 1001 doi:10.1029/2010PA002008.
 1002 Hendry, K. R., Andersen, M. B., 2013, The zinc isotopic composition of siliceous marine
 1003 sponges: investigating nature's sediment traps. *Chemical Geology* 354, 33-41.
 1004 Hendry, K. R., Georg, R. B., Rickaby, R. E. M., Robinson, L. F., Halliday, A. N., 2010, Deep
 1005 ocean nutrients during the Last Glacial Maximum deduced from sponge silicon
 1006 isotopic compositions. *Earth and Planetary Science Letters* 292, 290-300.
 1007 Hendry, K. R., Leng, M. J., Robinson, L. F., Sloane, H. J., Blusztjan, J., Rickaby, R. E. M.,
 1008 Georg, R. B., Halliday, A. N., 2011, Silicon isotopes in Antarctic sponges: an
 1009 interlaboratory comparison. *Antarctic Science* 23, 34-42.
 1010 Hendry, K. R., Rickaby, R. E. M., 2008, Opal (Zn/Si) ratios as a nearshore geochemical proxy
 1011 in coastal Antarctica. *Paleoceanography* 23, PA2218, doi:10.1029/2007PA001576.
 1012 Hendry, K. R., Robinson, L. F., 2012, The relationship between silicon isotope fractionation
 1013 in sponges and silicic acid concentration: modern and core-top studies of biogenic
 1014 opal. *Geochimica et Cosmochimica Acta* 81, 1-12.
 1015 Hendry, K. R., Robinson, L. F., McManus, J. F., Hays, J. D., in press, Silicon isotopes indicate
 1016 enhanced carbon export efficiency in the North Atlantic during deglaciation. *Nature*
 1017 *Communications*.
 1018 Hendry, K. R., Robinson, L. F., Meredith, M. P., Mulitza, S., Chiessi, C. M., and Arz, H.,
 1019 2012, Abrupt changes in high-latitude nutrient supply to the Atlantic during the last
 1020 glacial cycle. *Geology* 40 (2), 123-126.
 1021 Higginson, M. J., Altabet, M. A., 2004, Initial tests of the silicic acid leakage hypothesis using
 1022 sedimentary biomarkers. *Geophysical Research Letters* 31, L18303,
 1023 doi:10.1029/2004GL020511.
 1024 Holte, J., Talley, L. D., Chereskin, T. K., Sloyan, B.M., 2012, The role of air-sea fluxes in
 1025 Subantarctic Mode Water formation. *Journal of Geophysical Research* 117, C03040,
 1026 doi:10.1029/2011JC007798.
 1027 Horn, M. G., Beucher, C., Robinson, R. S., Brzezinski, M. A., 2011, Southern Ocean nitrogen
 1028 and silicon dynamics during the last deglaciation. *Earth and Planetary Science Letters*
 1029 310, 334-339.
 1030 Hutchins, D.A., DiTullio, G.R., Zhang, Y., Bruland, K.W., 1998. An iron limitation mosaic in
 1031 the California upwelling regime. *Limnology and Oceanography* 43 (6), 1037-1054.
 1032 Jaccard, S. L., Hayes, C. T., Martinez-Garcia, A., Hodell, D. A., Anderson, B. E., 2013, Two
 1033 modes of change in Southern Ocean productivity over the past million years. *Science*
 1034 339, 1419-1423.
 1035 Johnson, H. P., Hautala, S. L., Bjorklund, T. A., Zarnetske, M. R., 2006, Quantifying the

1036 North Pacific silica plume. *Geochemistry Geophysics Geosystems* 7, Q05011,
1037 doi:05010.01029/02005GC001065.

1038 Keigwin, L. D., 2004, Radiocarbon and stable isotope constraints on Last Glacial Maximum
1039 and Younger Dryas ventilation in the western North Atlantic. *Paleoceanography* 19,
1040 PA4012, doi:4010.1029/2004PA001029.

1041 Kemp, A. E. S., Pearce, R. B., Grigorov, I., Rance, J., Lange, C. B., Quilty, P., Salter, I., 2006,
1042 Production of giant marine diatoms and their export at oceanic frontal zones:
1043 implications for Si and C flux from stratified oceans. *Global Biogeochemical Cycles*
1044 20, doi: 10.1029/2006GB002698.

1045 Kienast, S. S., Kienast, M., Jaccard, S., Calvert, S. E., Francois, R., 2006, Testing the silica
1046 leakage hypothesis with sedimentary opal records from the eastern equatorial Pacific
1047 over the last 150 kyrs. *Geophysical Research Letters* 33, L15607,
1048 doi:15610.11029/12006GL026651.

1049 Koutavas, A., Sachs, J. P., 2008, Northern timing of deglaciation in the eastern equatorial
1050 Pacific from alkenone paleothermometry. *Paleoceanography* 23,
1051 doi:10.1029/2008PA001593.

1052 Kumar, N., Anderson, R.F., Mortlock, R.A., Froelich, P.N., Kubik, P., Dittrich-Hannen, B.,
1053 Suter, M., 1995, Increased biological productivity and export production in the glacial
1054 Southern Ocean. *Nature* 378, 675-680.

1055 Lal, D., Charles, C., Vacher, L., Goswami, J. N., Jull, A. J. T., McHargue, L., Finkel, R. C.,
1056 2006, Paleo-ocean chemistry records in marine opal: implications for fluxes of trace
1057 elements, cosmogenic nuclides (^{10}Be and ^{26}Al), and biological productivity.
1058 *Geochimica Cosmochimica Acta* 70, 3275-3289.

1059 Lambert, F., Delmonte, B., Petit, J.R., Bigler, M., Kaufmann, P.R., Hutterli, M.A., Stocer,
1060 T.F., Ruth, U., Steffensen, J.P., Maggi, V., 2008, Dust-climate couplings over the past
1061 800,000 years from the EPICA Dome C ice core. *Nature* 452, 616-619.

1062 Leng, M. J., Sloane, H. J., 2008, Combined oxygen and silicon isotope analysis of biogenic
1063 silica. *Journal of Quaternary Science* 23, 313-319.

1064 Maldonado, M., Navarro, L., Grasa, A., Gonzalez, A., Vaquerizo, I., 2011, Silicon uptake by
1065 sponges: a twist to understanding nutrient cycling on continental margins. *Nature*
1066 *Scientific Reports* 1, doi:10.1038/srep00030.

1067 Mangini, A., Godoy, J. M., Godoy, M. L., Kowman, R., Santos, G. M., Ruckelshausen, M.,
1068 Schroeder-Ritzrau, A., and Wacker, L., 2010, Deep sea corals off Brazil verify a
1069 poorly ventilated Southern Pacific Ocean during H1 and the Younger Dryas: *Earth and*
1070 *Planetary Science Letters*, v. 293, p. 269-276.

1071 Marchetti, A., Harrison, P.J., 2007. Coupled changes in the cell morphology and the
1072 elemental (C, N and Si) composition of the pennate diatom *Pseudo-nitzschia* due to
1073 iron deficiency. *Limnology and Oceanography* 52 (5), 2270-2284.

1074 Marinov, I., Gnanadesikan, A., Sarmiento, J. L., Toggweiler, J. R., Follows, M., Mignone, B.
1075 K., 2008, Impact of oceanic circulation on biological carbon storage in the ocean and
1076 atmospheric pCO₂. *Global Biogeochemical Cycles* 22, GB3007,
1077 doi:3010.1029/2007GB002958.

1078 Marinov, I., Gnanadesikan, A., Toggweiler, R., Sarmiento, J. L., 2006, The Southern Ocean
1079 biogeochemical divide. *Nature* 441, 964-968.

1080 Martin-Jezequel, V., Hildebrand, M., Brzezinski, M. A., 2003, Silicon metabolism in diatoms:
1081 Implications for growth, *Journal of Phycology* 36 (5), 821-840.

1082 Marshall, J., Speer, K., 2012, Closure of the meridional overturning circulation
1083 through Southern Ocean upwelling. *Nature Geosciences*, 5, 171-180.

1084 Matsumoto, K., Sarmiento, J. L., 2008, A corollary to the silicic acid leakage hypothesis.

1085 Paleocceanography 23, doi:10.1029/2007PA001515.

1086 Matsumoto, K., Sarmiento, J. L., Brzezinski, M. A., 2002, Silicic acid leakage from the
 1087 Southern Ocean: a possible explanation for glacial atmospheric pCO₂. *Global*
 1088 *Biogeochemical Cycles* 16, 1031.

1089 McClymont, E. L., Ganeshram, R. S., Pichevin, L. E., Talbot, H. M., van Dongen, B. E.,
 1090 Thunell, R. C., Haywood, A. M., Singarayer, J. S., Valdes, P. J., 2012, Sea-surface
 1091 temperature records of Termination I in the Gulf of California: Challenges for
 1092 seasonal and interannual analogies of tropical Pacific climate change,
 1093 *Paleocceanography* 27, doi:10.1029/2011PA002226.

1094 McManus, J. F., Francois, R., Gherardi, J.-M., Keigwin, L. D., Brown-Leger, S., 2004,
 1095 Collapse and rapid resumption of Atlantic meridional circulation linked to deglacial
 1096 climate changes. *Nature* 428, 834-837.

1097 Meckler, A. N., Sigman, D. M., Gibson, K. A., Francois, R., Martinez-Garcia, A., Jaccard, S.
 1098 L., Rohl, U., Peterson, L. C., Tiedemann, R., Haug, G. H., 2013, Deglacial pulses of
 1099 deep-ocean silicate into the subtropical North Atlantic Ocean. *Nature* 495, 495-498.

1100 Milligan, A. J., Varela, D. E., Brzezinski, M. A., Morel, F. M. M., 2004, Dynamics of silicon
 1101 metabolism and silicon isotopic discrimination in a marine diatom as a function of
 1102 pCO₂. *Limnology and Oceanography* 49, 322-329.

1103 Minoletti, F., Hermoso, M., Gressier, V., 2009, Separation of sedimentary micron-sized
 1104 particles for palaeocceanography and calcareous nannoplankton biogeochemistry.
 1105 *Nature Protocols* 4, 14-24.

1106 Moreno, A., Nave, S., Kuhlmann, H., Canals, M., Targarona, J., Freudenthal, T., Abrantes, F.
 1107 G., 2002, Productivity response in the North Canary Basin to climate changes during
 1108 the last 250,000 yr: a multi-proxy approach. *Earth and Planetary Science Letters* 196
 1109 (3-4) 147-159.

1110 Nelson, D. M., Anderson, R. F., Barber, R. T., Brzezinski, M. A., Buesseler, K. O., Chase, Z.,
 1111 Collier, R. W., Dickson, M.-L., Francois, R., Hiscock, M. R., Honjo, S., Marra, J.,
 1112 Martin, W. R., Sambrotto, R. N., Sayles, F. L., Sigman, D. E., 2002, Vertical budgets
 1113 for organic carbon and biogenic silica in the Pacific sector of the Southern Ocean,
 1114 1996-1998. *Deep-Sea Research II* 49, 1645-1674.

1115 Nelson, D. M., Treguer, P., Brzezinski, M. A., Leynaert, A., Queguiner, B., 1995, Production
 1116 and dissolution of biogenic silica in the ocean: revised global estimates, comparison
 1117 with regional data and relationship to biogenic sedimentation. *Global Biogeochemical*
 1118 *Cycles* 9, 359-372.

1119 Nozaki, Y., Yamamoto, Y., 2001, Radium 228 based nitrate fluxes in the eastern Indian Ocean
 1120 and the South China Sea and silica-induced "alkalinity pump" hypothesis. *Global*
 1121 *Biogeochemical Cycles* 15, 555-567.

1122 Opfergelt, S., Burton, K. W., Pogge von Strandmann, P. A. E., Gislason, S. R., Halliday, A.
 1123 N., 2013, Riverine silicon isotope variations in glaciated basaltic terrains: Implications
 1124 for the Si delivery to the ocean over glacial-interglacial intervals. *Earth and Planetary*
 1125 *Science Letters* 369-370, 211-219.

1126 Pahnke, K., Zahn, R., 2005, Southern Hemisphere water mass conversion linked with North
 1127 Atlantic climate variability. *Science* 307, 1741-1746.

1128 Pahnke, K., Goldstein, S. L., Hemming, S. R., 2008, Abrupt changes in Antarctic Intermediate
 1129 Water circulation over the past 25,000 years. *Nature Geoscience* 1, 870-874.

1130 Pena, L., Goldstein, S. L., Hemming, S. R., Jones, K. M., Calvo, E., Pelejero, C., Cacho, I.,
 1131 2013, Rapid changes in meridional advection of Southern Ocean intermediate waters
 1132 to the tropical Pacific during the last 30 kyr. *Earth and Planetary Science Letters* 368,
 1133 20-32.

1134 Pichat, S., Sims, K. W. W., Francois, R., McManus, J. F., Leger, S. B., Albarede, F., 2004,
1135 Lower export production during glacial periods in the equatorial Pacific from
1136 ($^{231}\text{Pa}/^{230}\text{Th}$)_{xs,0} measurements in deep-sea sediments. *Paleoceanography* 19, PA4023,
1137 doi:4010.1029/2003PA000994.

1138 Pichevin, L. E., Ganeshram, R. S., Francavilla, S., Arellano-Torres, E., Pedersen, T. F.,
1139 Beaufort, L., 2010, Interhemispheric leakage of isotopically heavy nitrate in the
1140 eastern tropical Pacific during the last glacial period. *Paleoceanography* 25, PA1204,
1141 doi:1210.1029/2009PA001754.

1142 Pichevin, L. E., Reynolds, B. C., Ganeshram, R. S., Cacho, I., Pena, L., Keefe, K., Ellam, R.
1143 M., 2009, Enhanced carbon pump inferred from relaxation of nutrient limitation in the
1144 glacial ocean. *Nature* 459, 1114-1117.

1145 Piotrowski, A. M., Goldstein, S. L., Hemming, S. R., Fairbanks, R. G., Zylberberg, D. R.,
1146 2008, Oscillating glacial northern and southern deep water formation from combined
1147 neodymium and carbon isotopes: *Earth and Planetary Science Letters* 272, 394-405.

1148 Pondaven, P., Ragueneau, O., Tréguer, P., Hauvespre, A., Dezileau, L., Reyss, J. L., 2000,
1149 Resolving the "opal paradox" in the Southern Ocean. *Nature* 405, 168-172.

1150 Reincke, T., Barthel, D., 1997, Silica uptake kinetics of *Halichondria panicea* in Kiel Bight.
1151 *Marine Biology* 129, 591-593.

1152 Ren, H., Brunelle, B. G., Sigman, D. M., Robinson, R. S., 2013, Diagenetic aluminium uptake
1153 into diatom frustules and the preservation of diatom-bound organic nitrogen. *Marine*
1154 *Chemistry* 155, 92-102.

1155 Reynolds, B. C., 2009, Modeling the modern marine $\delta^{30}\text{Si}$ distribution: *Global*
1156 *Biogeochemical Cycles* 23, GB2015, doi:2010.1029/2008GB003266.

1157 Reynolds, B. C., Frank, M., and Halliday, A. N., 2006, Silicon fractionation during nutrient
1158 utilization in the North Pacific. *Earth and Planetary Science Letters* 244, 431-443.

1159 Richaud, M., Loubere, P., Pichat, S., Francois, R., 2007, Changes in opal flux and the rain
1160 ratio during the last 50,000 years in the equatorial Pacific. *Deep-Sea Research II:*
1161 *Topical Studies in Oceanography* 54 (5-7), 762-771.

1162 Rickaby, R. E. M., Bard, E., Sonzogni, C., Rostek, F., Beaufort, L., Barker, S., Rees, G.,
1163 Schrag, D. P., 2007, Coccolith chemistry reveals secular variations in the global ocean
1164 carbon cycle? *Earth and Planetary Science Letters* 253 (1-2), 83-95.

1165 Roberts, N. L., Piotrowski, A. M., McManus, J. F., Keigwin, L. D., 2010, Synchronous
1166 deglacial overturning and water mass source changes. *Science* 327, 75-78.

1167 Robinson, L. F., Adkins, J. F., Keigwin, L. D., Southon, J., Fernandez, D. P., Wang, S.-L.,
1168 Scheirer, D. S., 2005a, Radiocarbon variability in the western North Atlantic during
1169 the last deglaciation. *Science* 310, 1469-1473.

1170 Robinson, R. S., Brunelle, B. G., Sigman, D. M., 2004, Revisiting nutrient utilization in the
1171 glacial Antarctic: evidence from a new method for diatom-bound N isotope analysis:
1172 *Paleoceanography*, v. 19, p. doi:10.1029/2003PA000996.

1173 Robinson, R. S., Sigman, D. M., DiFiore, P. J., Rohde, M. M., Mashiotto, T. A., and Lea, D.
1174 W., 2005b, Diatom-bound $^{15}\text{N}/^{14}\text{N}$: New support for enhanced nutrient consumption
1175 in the ice age subantarctic. *Paleoceanography* 20 (3), doi:10.1029/2004PA001114.

1176 Romero, O. E., 2010, Changes in style and intensity of production in the Southeastern
1177 Atlantic over the last 70,000 yr. *Marine Micropaleontology* 74 (1-2), 15-28.

1178 Romero, O. E., Kim, J.-H., Donner, B., 2008, Submillennial-to-millennial variability of diatom
1179 production off Mauritania, NW Africa, during the last glacial cycle. *Paleoceanography*
1180 23, PA3218, doi:3210.1029/2008PA001601.

1181 Romero, O. E., Leduc, G., Vidal, L., Fischer, G., 2011, Millennial variability and long-term
1182 changes of the diatom population in the eastern equatorial Pacific during the last

1183 glacial cycle. *Paleoceanography* 26, doi:10.1029/2010PA002099.

1184 Sarmiento, J. L., Gruber, N., Brzezinski, M. A., Dunne, J. P., 2004, High-latitude controls of
 1185 thermocline nutrients and low latitude biological productivity. *Nature* 427, 56-60.

1186 Shemesh, A., 1989, Late Cenozoic Ge/Si record of marine biogenic opal: implications for
 1187 variations of riverine fluxes to the ocean. *Paleoceanography* 4, 221-234.

1188 -, 1995, Late Pleistocene oxygen isotope records of biogenic silica from the Atlantic sector of
 1189 the Southern Ocean. *Paleoceanography* 10, 179-196.

1190 Sigman, D. M., Hain, M. P., Haug, G. H., 2010, The polar ocean and glacial cycles in
 1191 atmospheric CO₂ concentration. *Nature* 466, 47-55.

1192 Spero, H. J., Lea, D. W., 2002, The cause of carbon isotope minimum events on glacial
 1193 terminations. *Science* 296, 522-525.

1194 Sutton, J., Varela, D., Brzezinski, M. A., Beucher, C., 2013, Species-dependent silicon isotope
 1195 fractionation by marine diatoms. *Geochimica et Cosmochimica Acta* 104, 300-309.

1196 Takeda, S., 1998, Influence of iron availability on nutrient consumption ratio of diatoms in
 1197 oceanic waters. *Nature* 393 (6687), 774-777.

1198 Thornalley, D. J. R., Barker, S., Broecker, W. S., Elderfield, H., McCave, I. N., 2011, The
 1199 deglacial evolution of North Atlantic deep convection. *Science* 331 (6014), 202-205.

1200 Toggweiler, R., 1999, Variation of atmospheric CO₂ by ventilation of the ocean's deepest
 1201 water. *Paleoceanography* 14, 571-588.

1202 Tréguer, P., De la Rocha, C. L., 2013, The world ocean silica cycle. *Annual Review of Marine*
 1203 *Science* 5, 477-501.

1204 Tréguer, P., Nelson, D. M., Van Bennekom, A. J., DeMaster, D. J., Leynaert, A., Quéguiner,
 1205 B., 1995, The silica balance in the world ocean: a re-estimate. *Science* 268, 375-379.

1206 Varela, D. E., Pride, C. J., Brzezinski, M. A., 2004, Biological fractionation of silicon
 1207 isotopes in Southern Ocean surface waters. *Global Biogeochemical Cycles* 18,
 1208 doi:10.1029/2003GB002140.

1209 Vink, A., Ruhlemann, C., Zonneveld, K. A. F., Mulitza, S., Huls, M., Willems, H., 2001,
 1210 Shifts in the position of the North Equatorial Current and rapid productivity changes
 1211 in the western Tropical Atlantic during the last glacial. *Paleoceanography* 16 (5), 479-
 1212 490.

1213 Wetzel, F., de Souza, G.F., Reynolds, B.C., in review, Silicon isotope effects during diatom
 1214 dissolution and their sensitivity to sample composition: *Geochimica Cosmochimica*
 1215 *Acta*.

1216 Wille, M., Sutton, J., Ellwood, M. J., Sambridge, M., Maher, W., Eggins, S., Kelly, M., 2010,
 1217 Silicon isotopic fractionation in marine sponges: a new model for understanding
 1218 silicon isotopic fractionation in sponges. *Earth and Planetary Science Letters* 292,
 1219 doi:10.1016/j.epsl.2010.1001.1036.

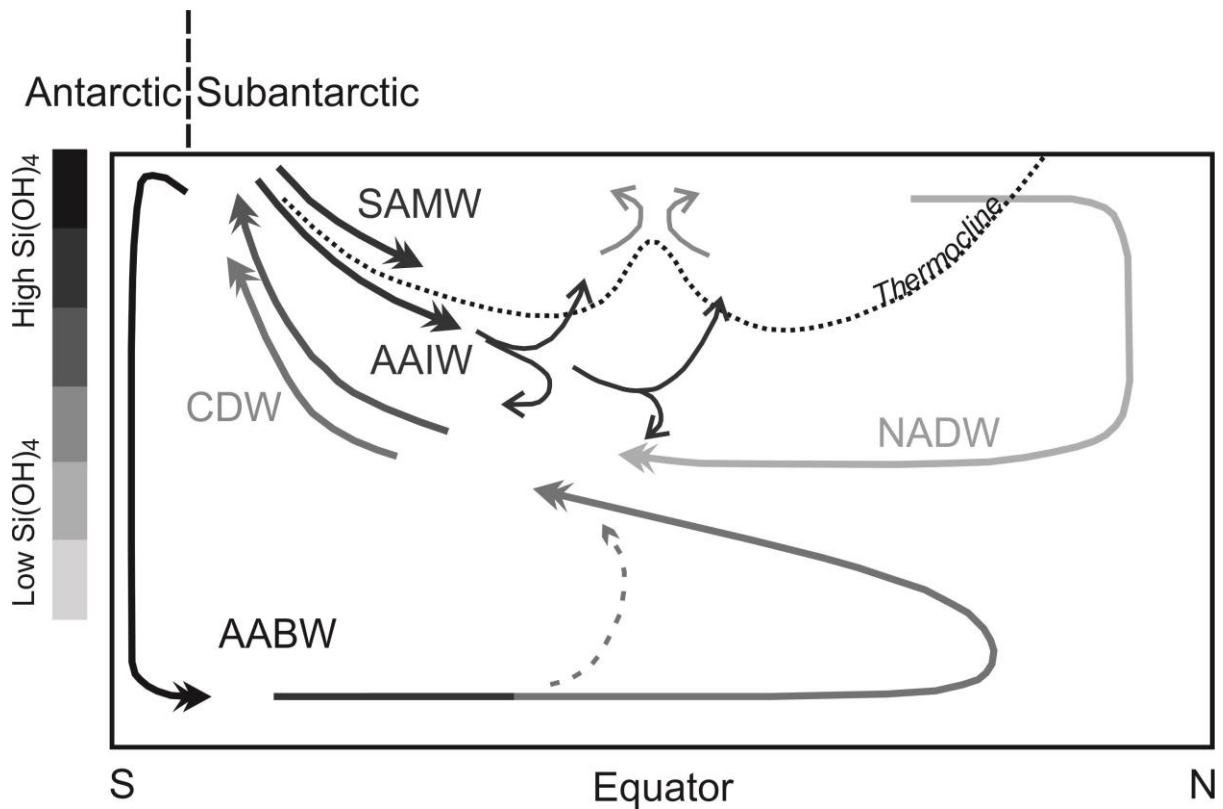
1220 Wischmeyer, A. G., De La Rocha, C., Maier-Raimer, E., Wolf-Gladrow, D. A., 2003, Control
 1221 mechanisms for the oceanic distribution of silicon isotopes: *Global Biogeochemical*
 1222 *Cycles*, v. 17, p. doi:10.1029/2002GB002022.

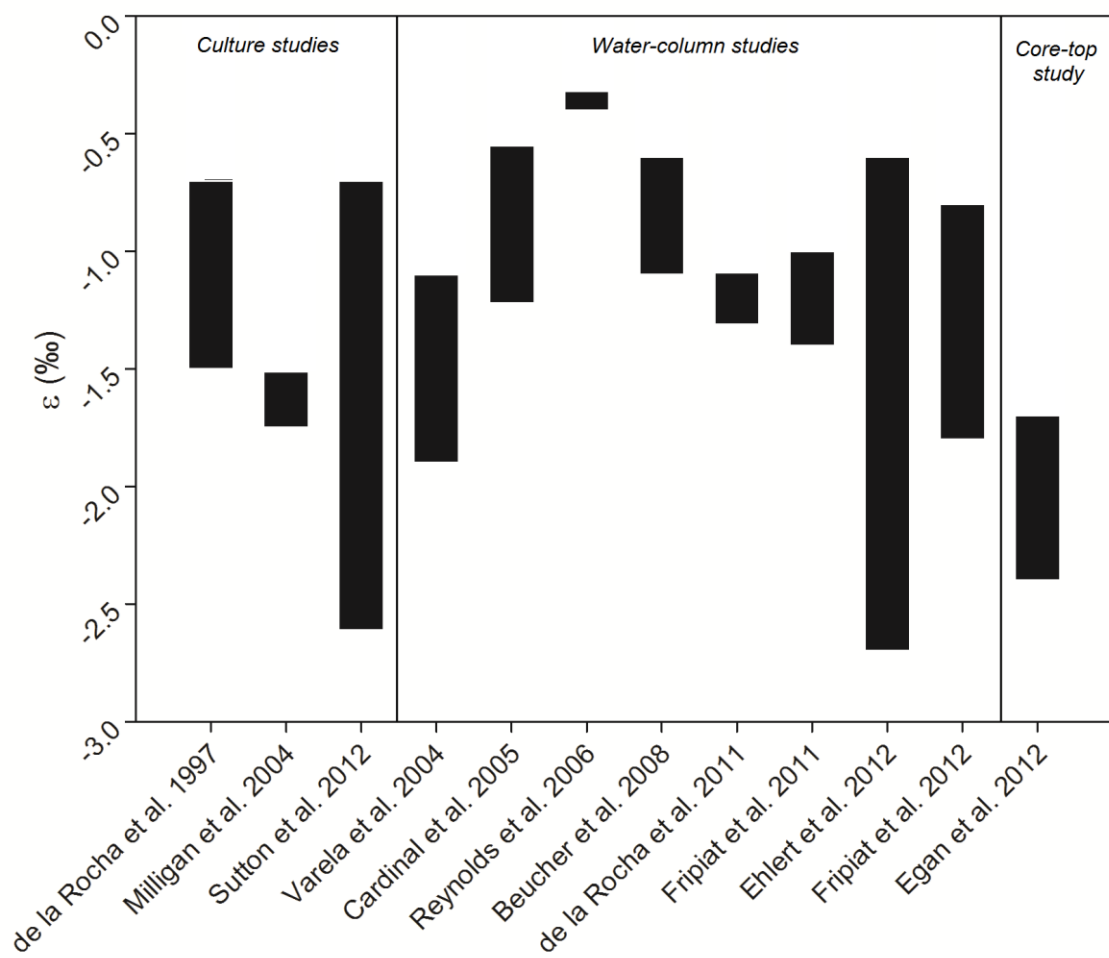
1223 Wu, S., Ding, T., Meng, X., Bai, L., 1997, Determination and geological implication of O-Si
 1224 isotope of the sediment core in the CC area, the Pacific Ocean. *Chinese Science*
 1225 *Bulletin* 42, 1462-1465.

1226 Xie, R. C., Marcantonio, F., Schmidt, M. W., 2012, Deglacial variability of Antarctic
 1227 Intermediate Water penetration into the North Atlantic from authigenic neodymium
 1228 isotope ratios. *Paleoceanography* 27 (3) doi:10.1029/2012/PA002337.

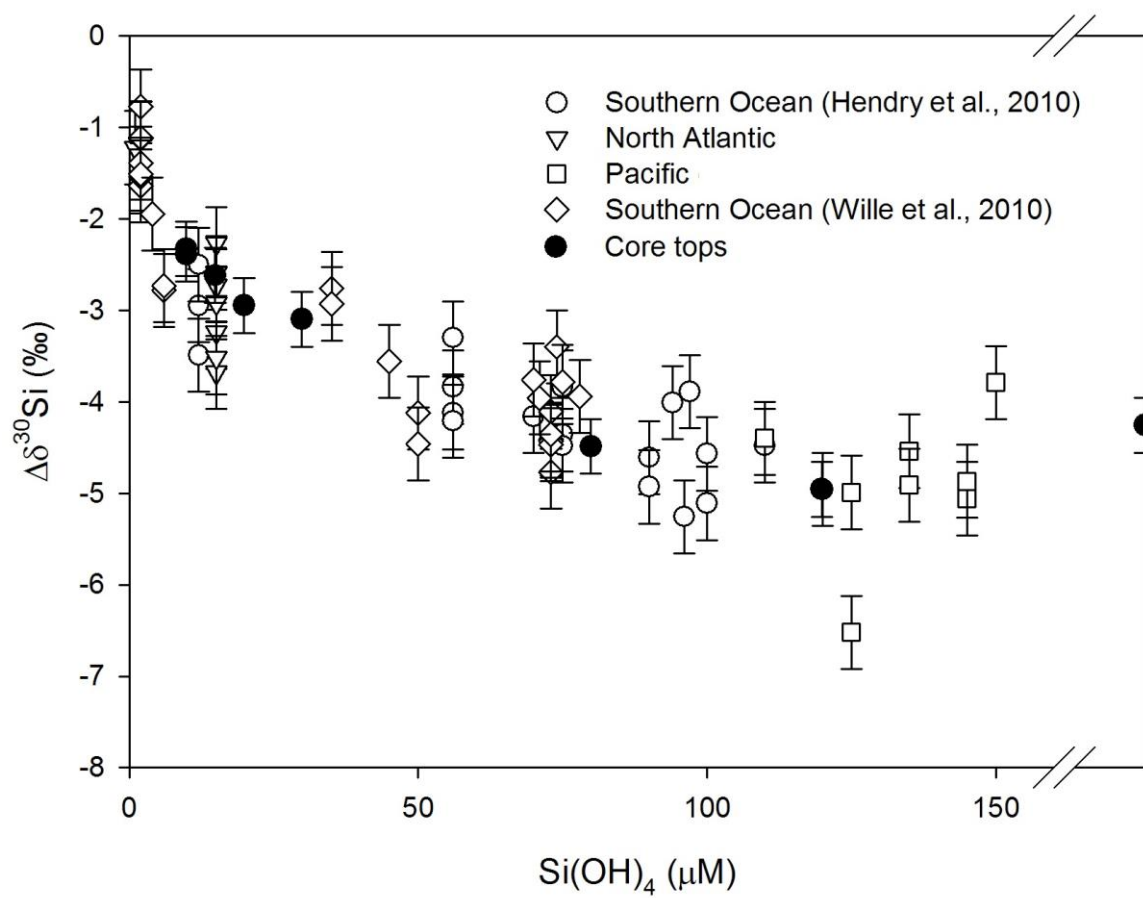
1229 Xiong, Z., Li, T., Crosta, X., Algeo, T., Chang, F., Zhai, B., 2013, Potential role of giant

marine diatoms in sequestration of atmospheric CO₂ during the Last Glacial
Maximum: $\delta^{13}\text{C}$ evidence from laminated *Ethmodiscus rex* mats in tropical West
Pacific. Global and Planetary Change 108, 1-14.
Zhai, B., Li, T., Chang, F., Cao, Z., 2009, Vast laminated diatom mat deposits from the west
low-latitude Pacific Ocean in the last glacial period: Chinese Science Bulletin 54 (23),
4529-4533.
Ziegler, K., Chadwick, O. A., Brzezinski, M. A., Kelly, E. F., 2005, Natural variations of $\delta^{30}\text{Si}$
ratios during progressive basalt weathering, Hawaiian Islands. Geochimica et
Cosmochimica Acta 69 (19), 4597-4610.

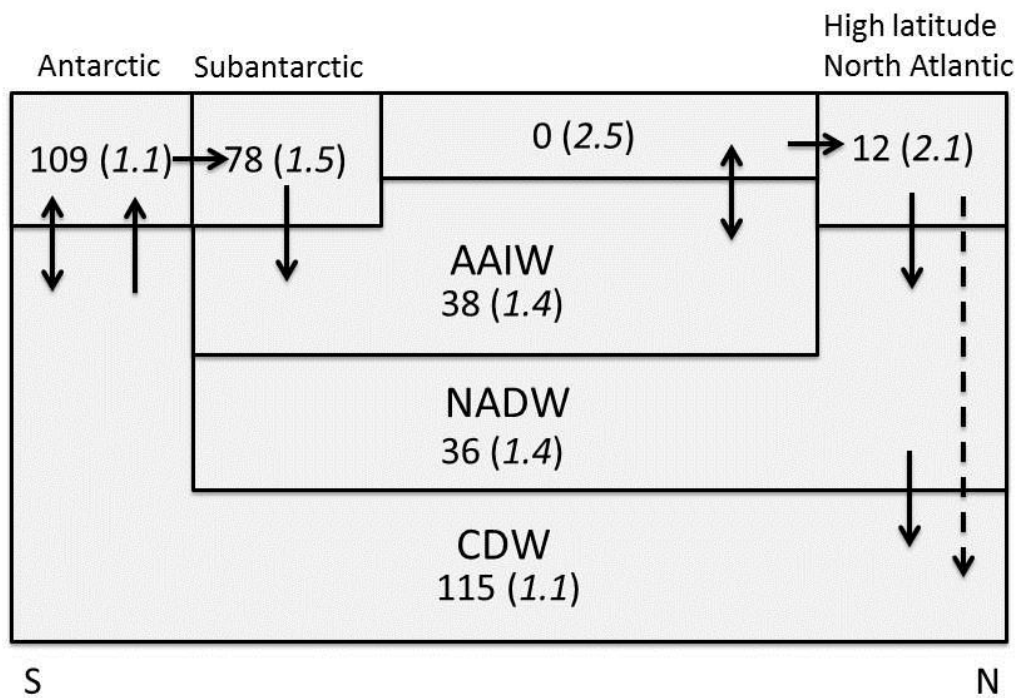




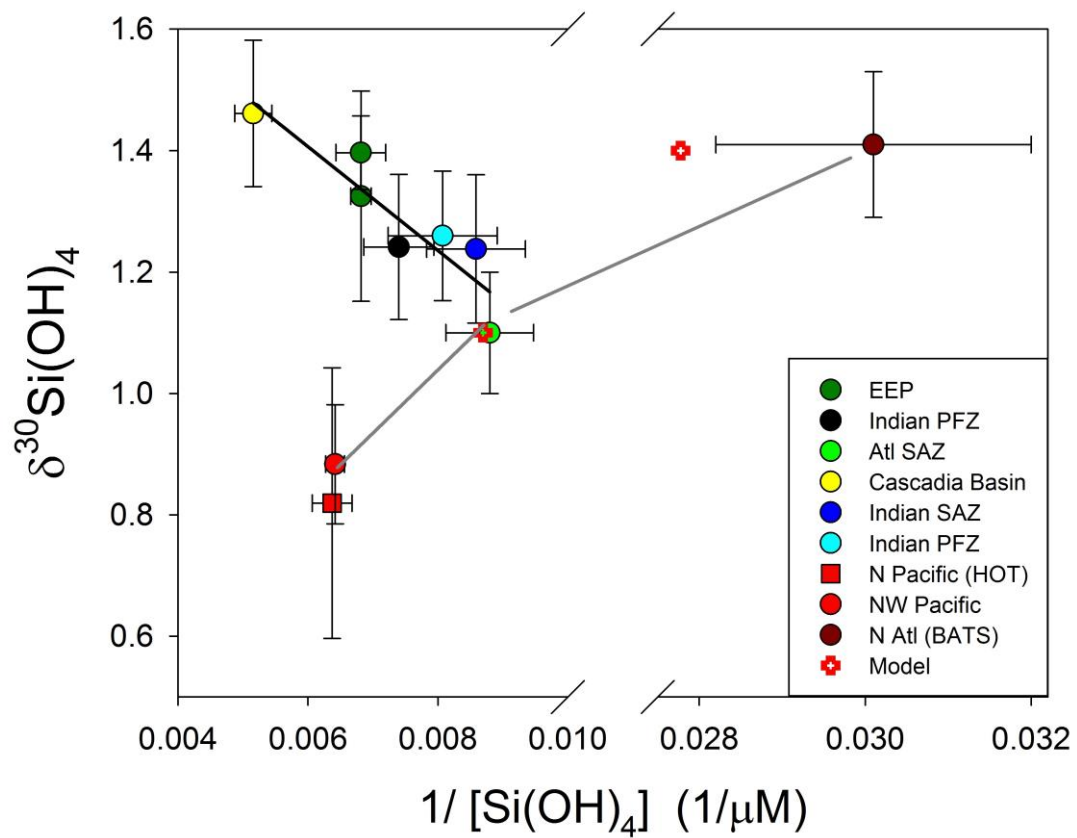
1242



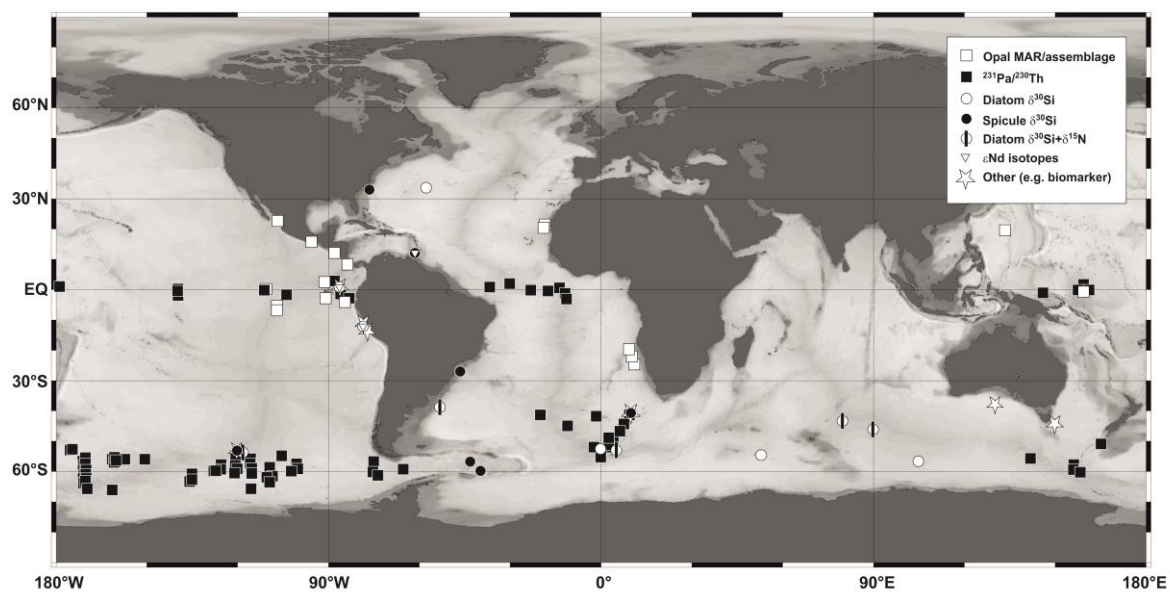
1243



1244



1245



1246

